Extragalactic Astronomy

Lecture 8: The Milky Way
Bulge, Disk (thin & Thick),
Halo (stars & globular clusters)

Structure of the bulge

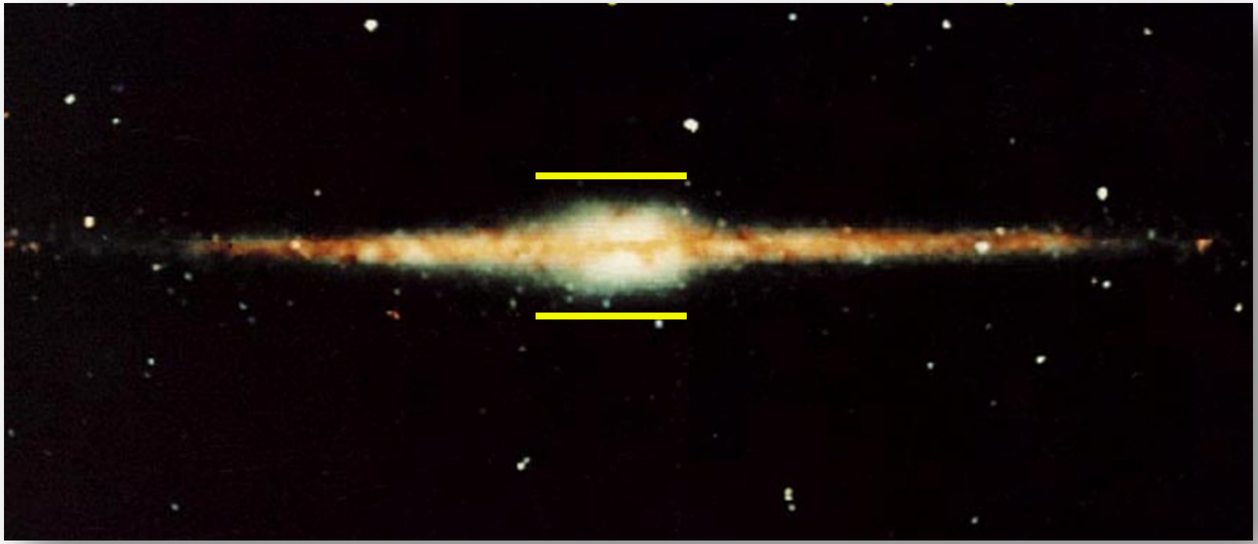

- Note that the left side is larger (near side) than the right side (extremity of the bar)
- Show that there is a bar in the center

Structure of the bulge

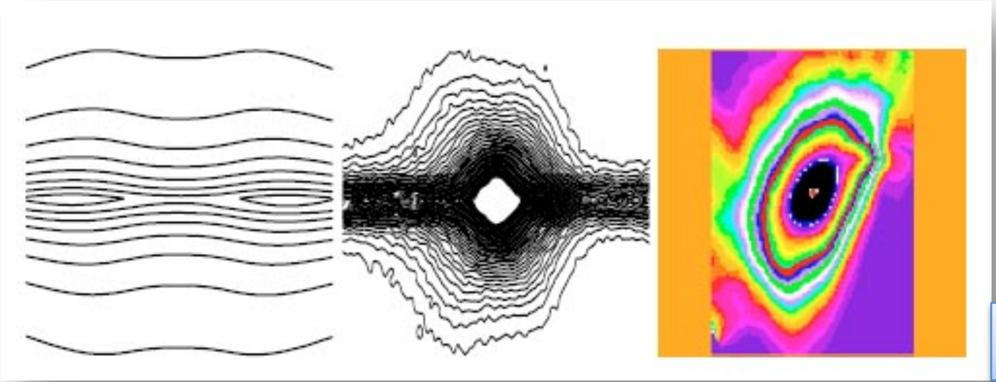

Star counts – 2MASS

Lopez-Corredoira et al. 2005

- (left): 2MASS star counts in the central parts of the MW
- (center): Counts minus the disk contribution
- (right): cut at z = 1440 pc

Unbarred and barred galaxies

Formation of the bulge

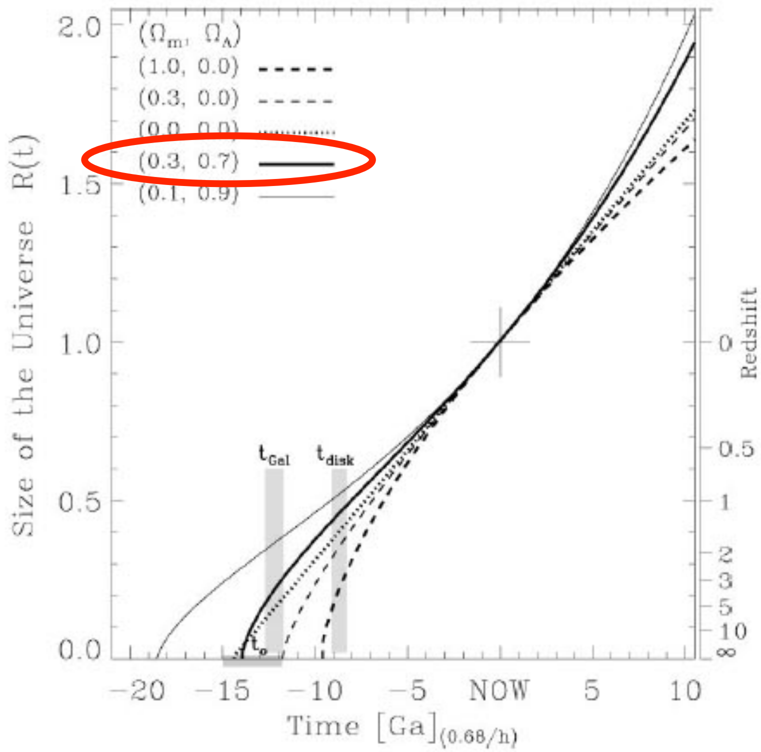

Figure 1 Look-back time as a function of redshift and the size of the Universe (Lineweaver 1999) for five different world models. The approximate ages of the Galactic halo and disk are indicated by hatched regions.

- Formation of the bulge
  12.5 < t_{form} < 9 Gy
- Formation first epoch
  t_{form} ~ 12.5 Gy
- Formation by secular evolution
  t_{form} ~ 9 Gy

Freeman & Bland-Hawthorn 2002

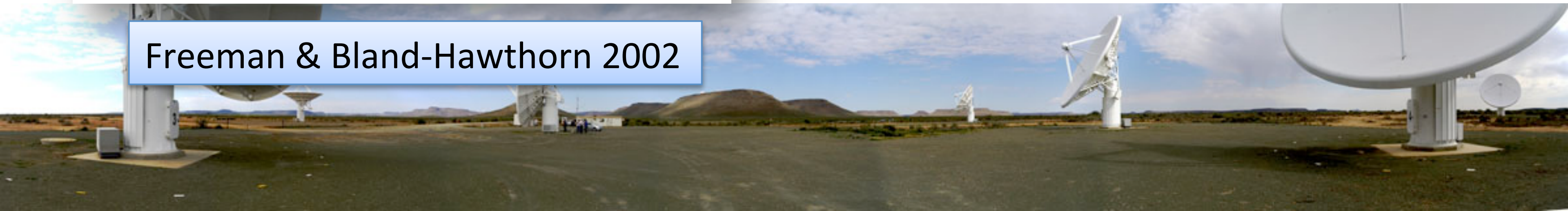

Formation of the bulge

Secular evolution
Barred Spiral

Star formation

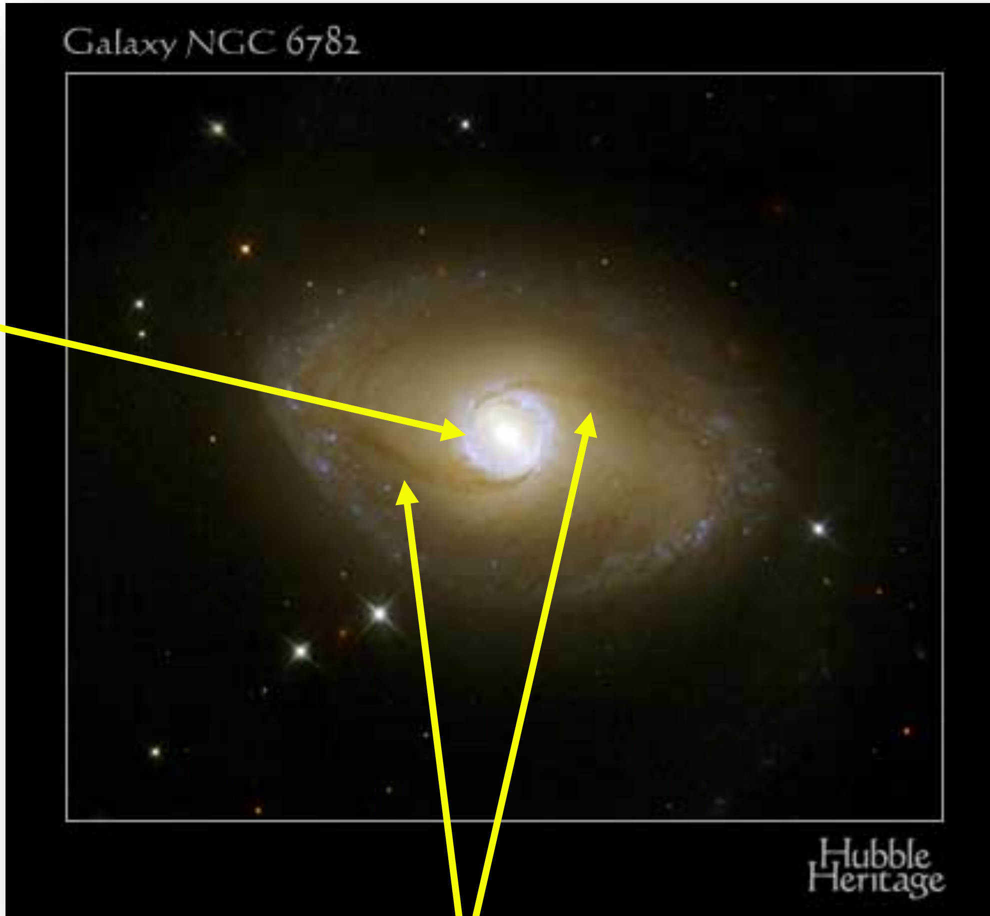

Matter falling on the bulge

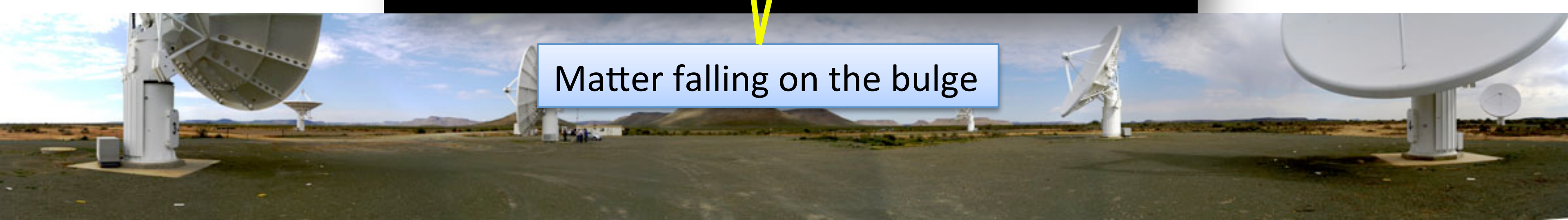

Formation of the bulge – NGC 1097

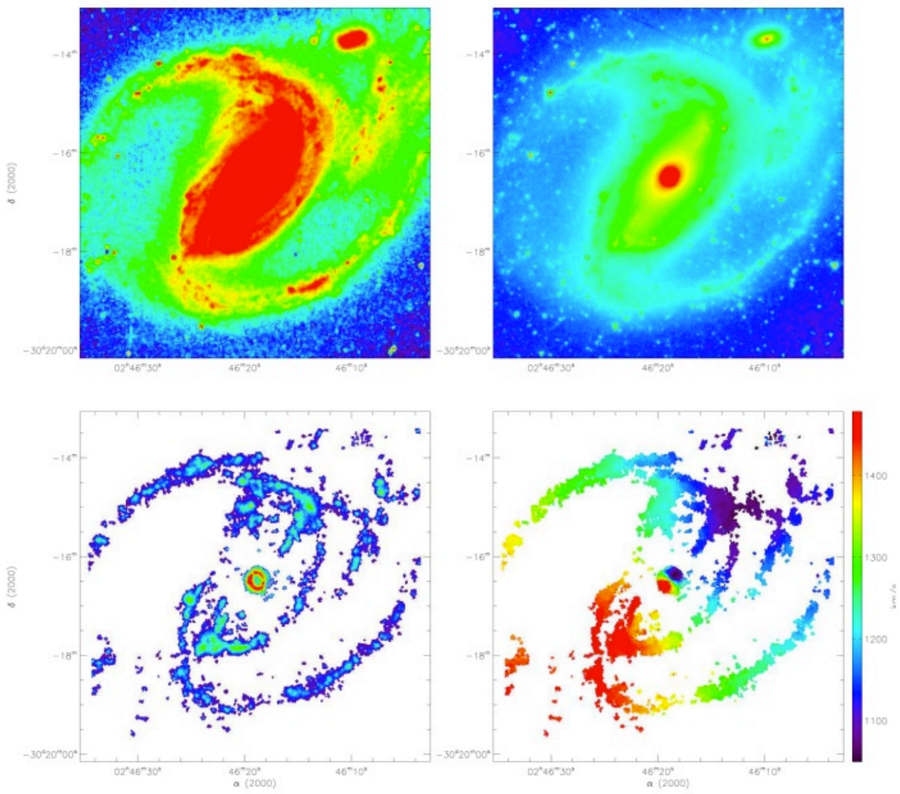

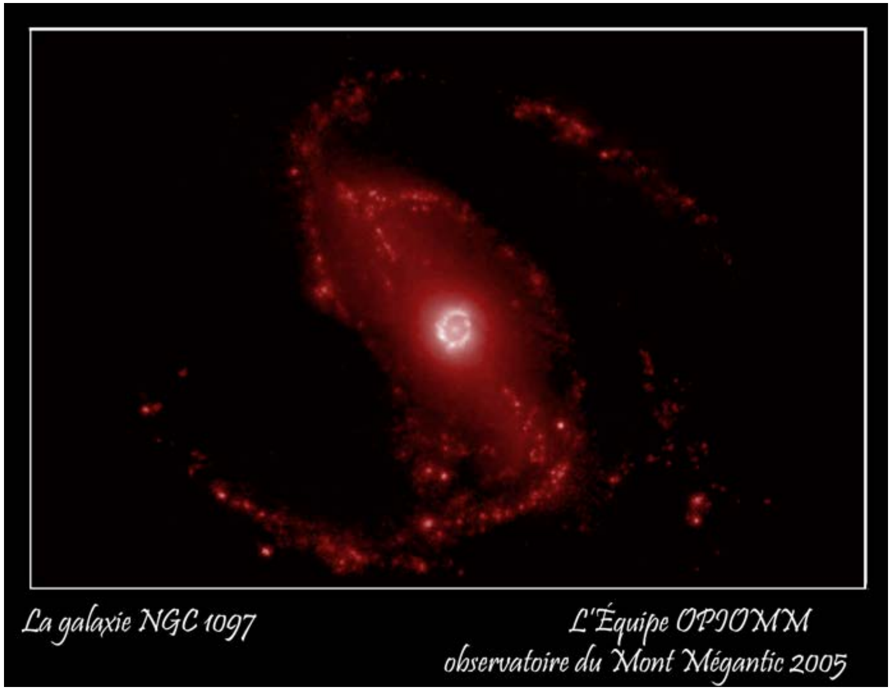

Formation of the bulge

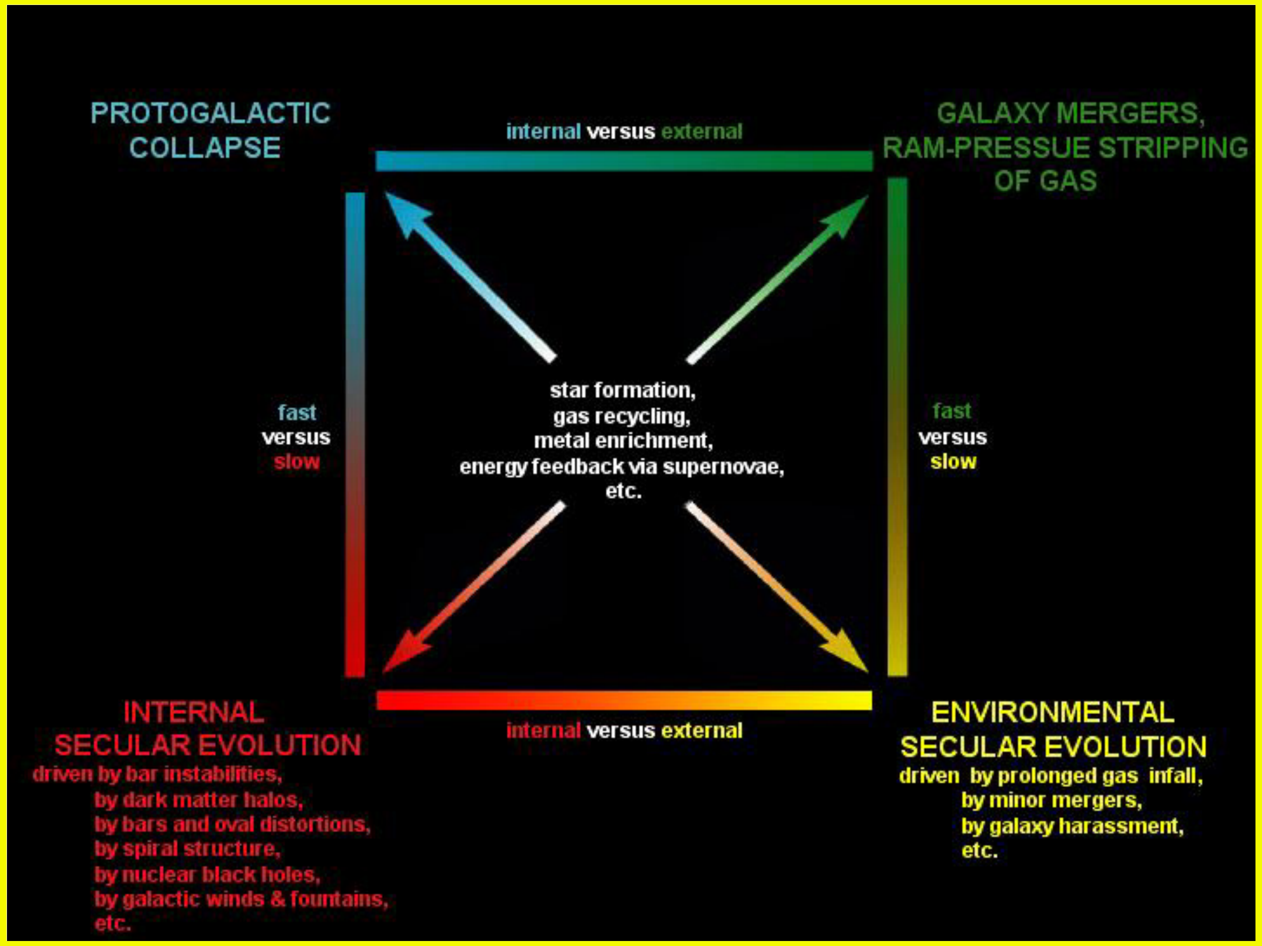

Kormendy 2004

Formation of the bulge

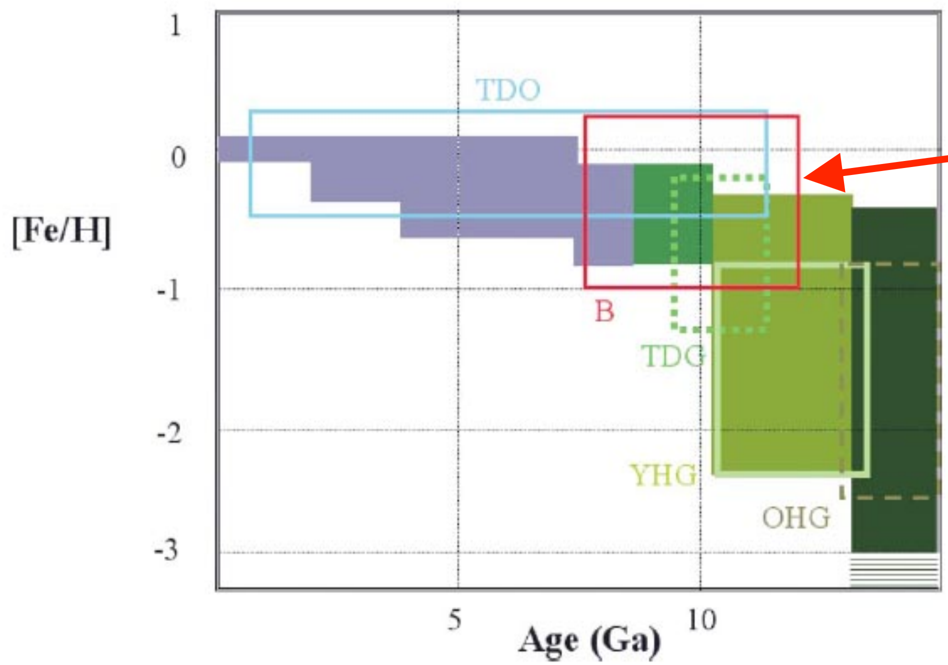

Figure 2 The age-metallicity relation of the Galaxy for the different components (see text): TDO—thin disk open clusters; TDG—thick disk globulars; B—bulge; YHG—young halo globulars; OHG—old halo globulars. The blue corresponds to thin disk field stars, the green to thick disk field stars, and the black shows the distribution of halo field stars extending down to [Fe/H] = −5.

Freeman & Bland-Hawthorn 2002

Profile of the bulge

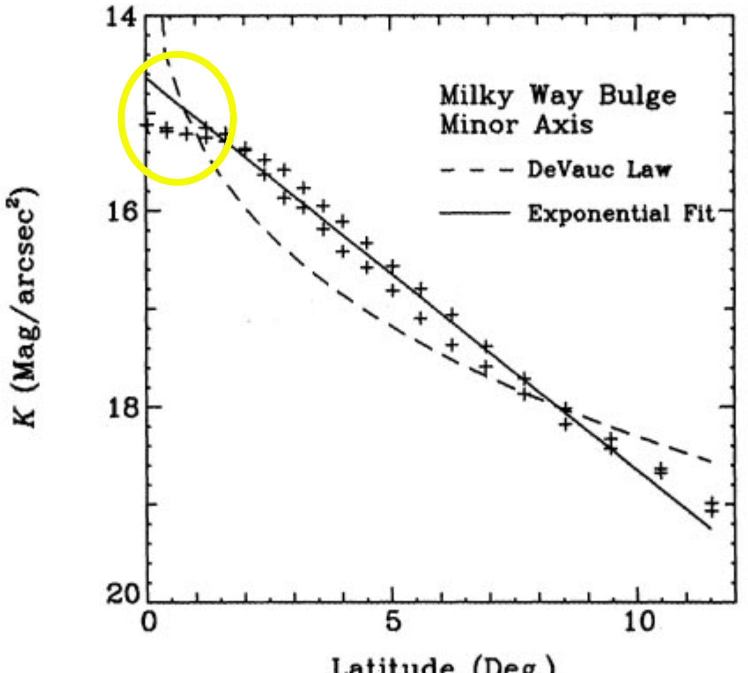

FIG. 1.—Bulge minor-axis profile, show both an exponential fit and the profile predicted by the spheroid model of de Vaucouleurs & Pence (1978); the latter profile assumes $V-K=3.2$.

- Bulge don't follow the de Vauc. $R^{1/4}$ law
- Bulge follow an exponential law, but not in the center

Profile of the bulge

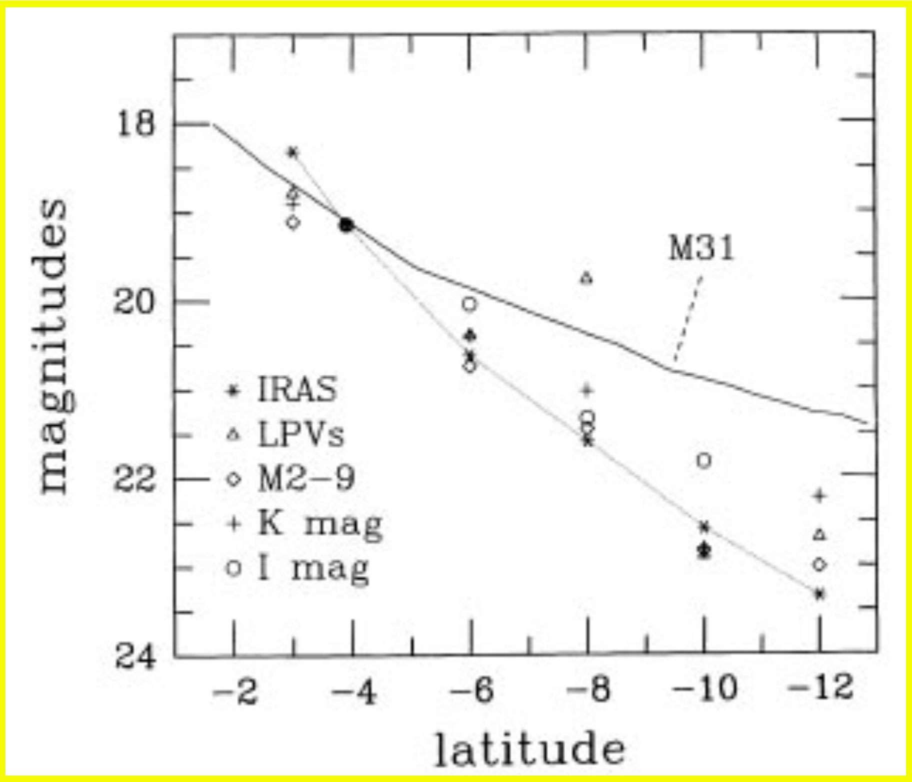

- Bulge of the MW is fainter than the one of M31
- MW is a later morphological type than M31 (Sbc vs Sb)

Kinematics of the bulge

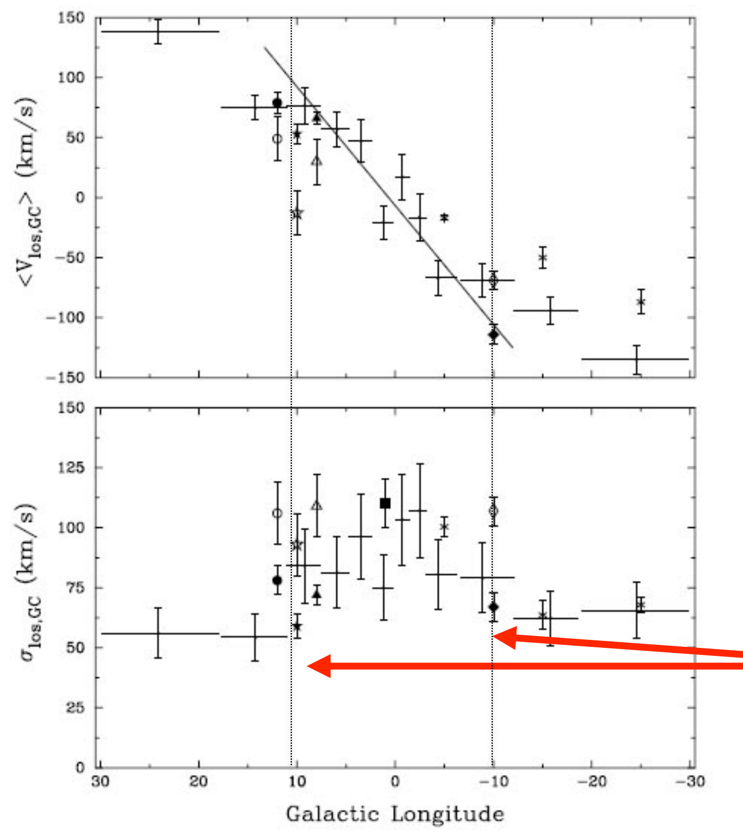

FIG. 13.—Mean galactocentric velocities V (*top panel*) and velocity dispersions σ (*lower panel*) vs. longitude for PNs in the Survey

- The bulge of the MW is in rotation as any other bulge
- Kinematics from K giants & PNs
- Bulge ends $|l| < +/- 10^o$

Metallicity of the bulge

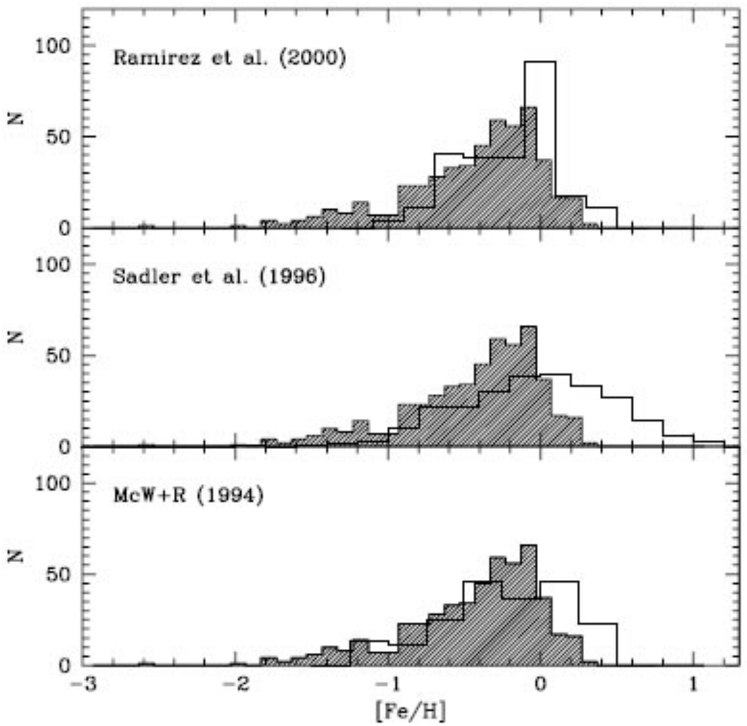

Fig. 14. Comparison between the bulge MD derived from Fig. 12 (shaded histogram) and those derived with spectroscopic surveys.

Zoccali et al. 2003:

1. No trace of very young populations
2. Metallicity of the bulge peaks close to the solar value
3. There is a clear cut-off for [Fe/H] > 0
4. A longer tail for small metallicity for [Fe/H] < -1

Galactic center (optical)

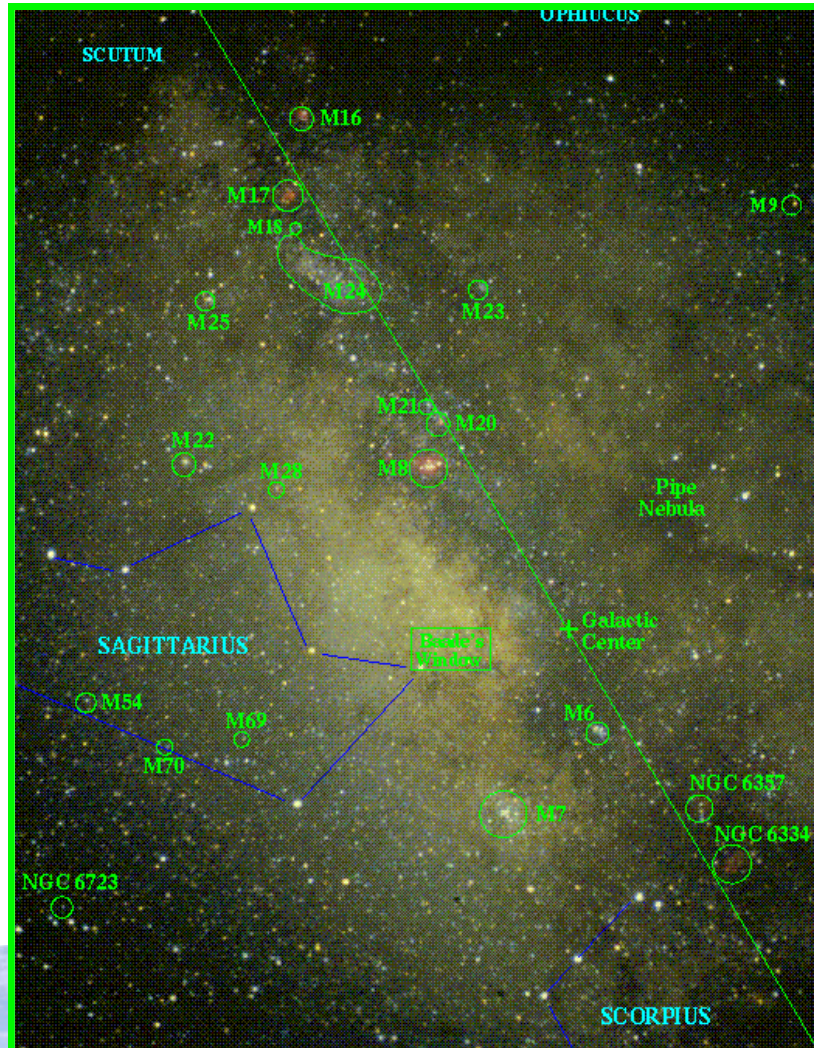

Galactic center (IR)

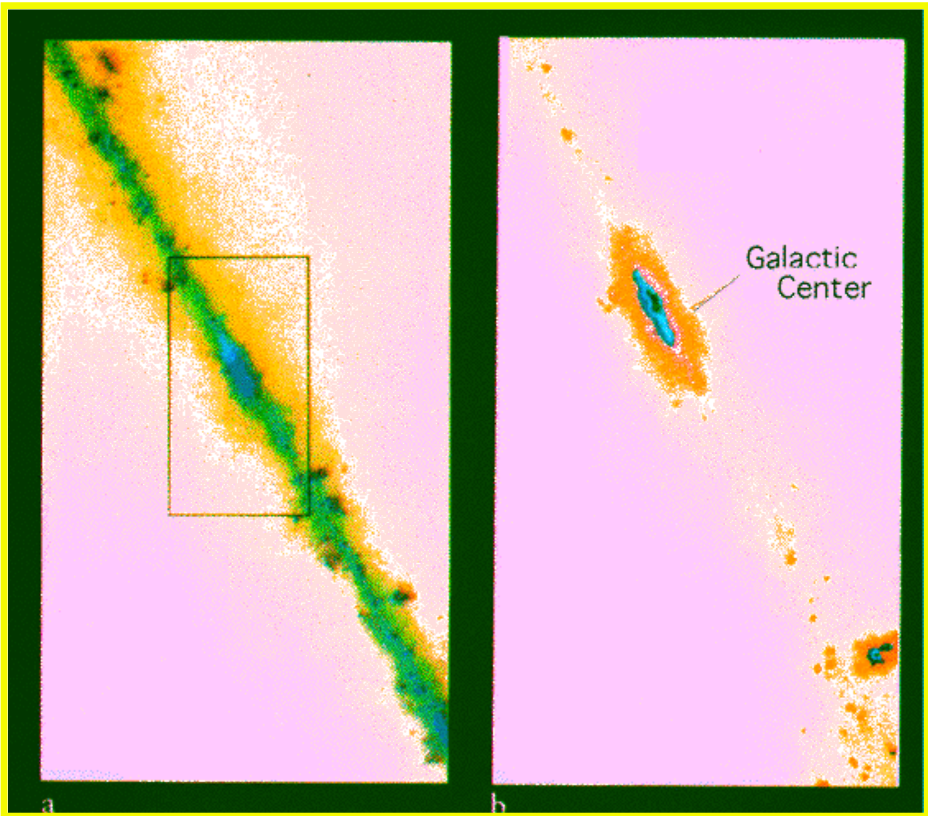

- IRAS images of the central regions of the Galaxy.
- IR emission due to dust heated by the neighboring stars

Galactic center (radio – 90cm)

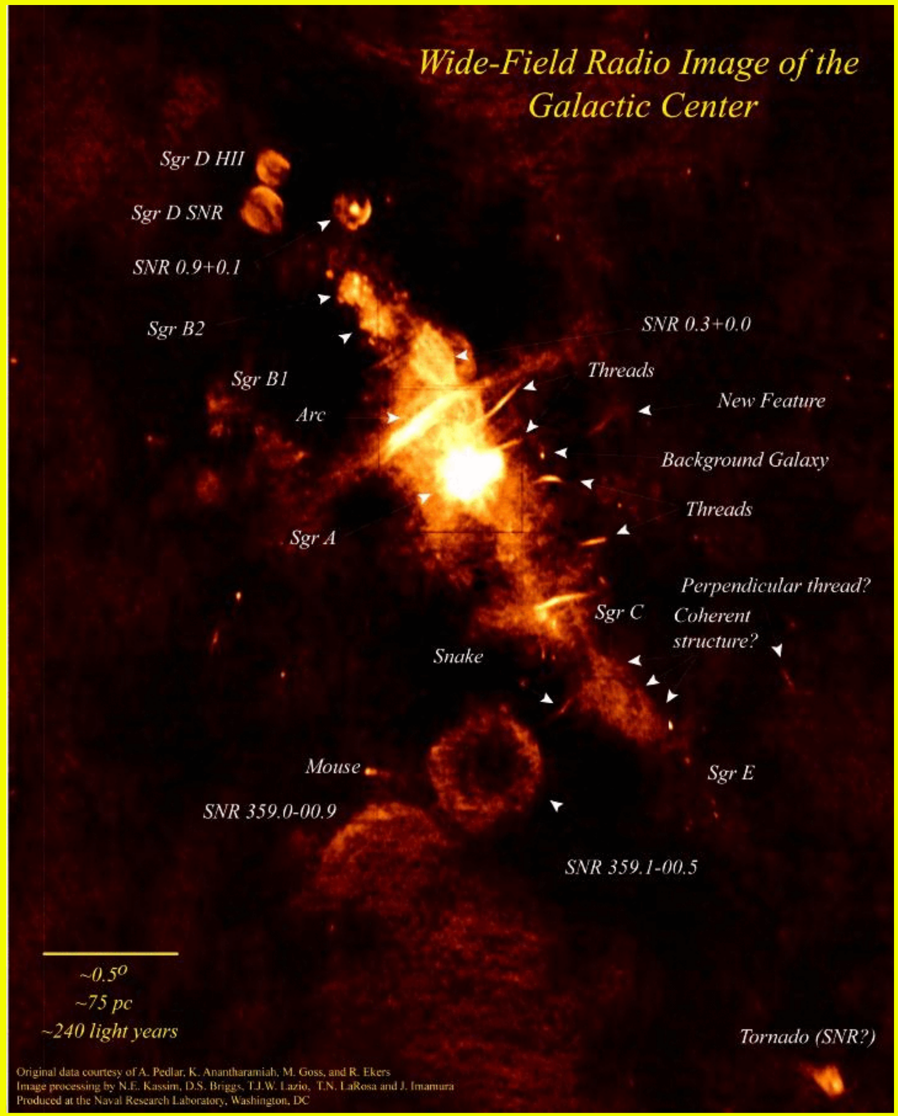

Galactic center

- Image HKL of the galactic center. The BH is close to the center of the box
- Inside a few light-years, we find a dense cluster of 10000 stars & a black hole of ~ 10^6 M_{sun}

Galactic center

- Central regions (0.3 pc) in IR (1.6, 2.2 & 3.8μm)
- Sgr A* is near the center but not very bright in IR
- Most of the stars are young and massive
- Spectroscopy shows that they are super-luminous giants of only a few 10 x 10^6 years

Galactic center (dynamics)

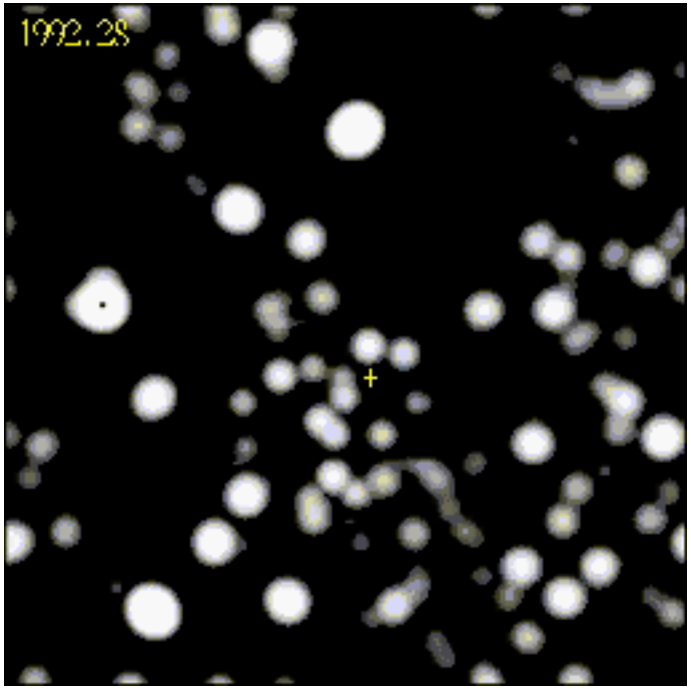

Proper motions around Sgr A+

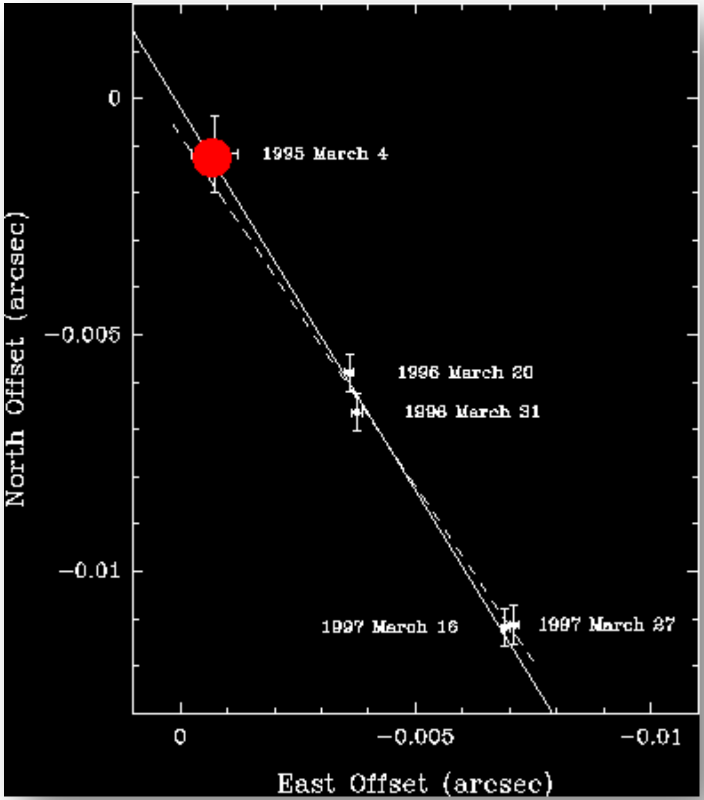

Correction for the sun motion

Galactic center (dynamics)

- Time resolved astrometry (period~15 years) gives good data on proper motions of stars near the galactic center
- Observations show that many stars at distances ~30 light-days move on Keplerian orbits
- From those orbits, distances Earth-Sgr A* and the mass of Sgr A* may be calculated

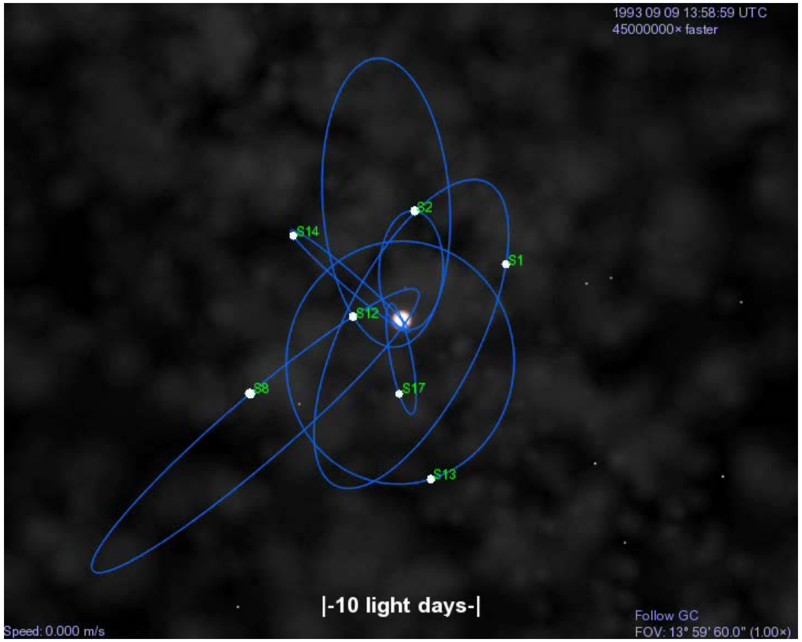

Central BH of the MW

- Most galaxies have a BH in their center
- Ghez et al.2005

  Mass = 3.7 +/-0.2 x 10^6 M_{sun} $[r_0/(8\ kpc)]^3$
- Schödel et al. 2003

  Mass = 3.3 +/-0.7 x 10^6 M_{sun} $[r_0/(8\ kpc)]^3$

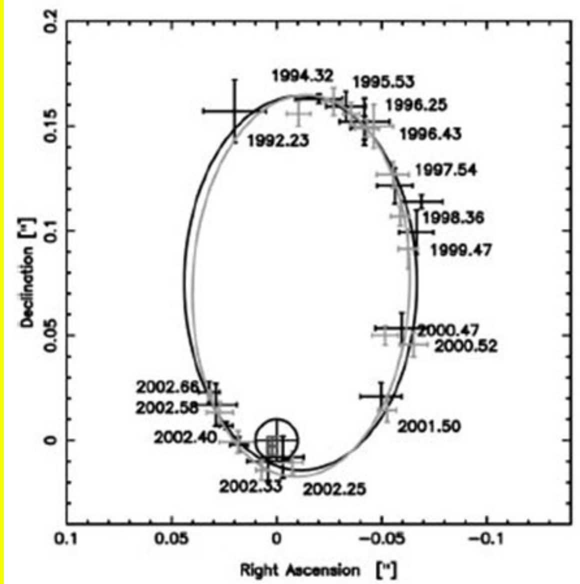

proper motion of star close to Gal Centre black hole, Schoedel et al (2003)

Radio Emission from Sgr A*

Radio image at 20 cm showing large scale filaments from the synchrotron emission along the magnetic field lines

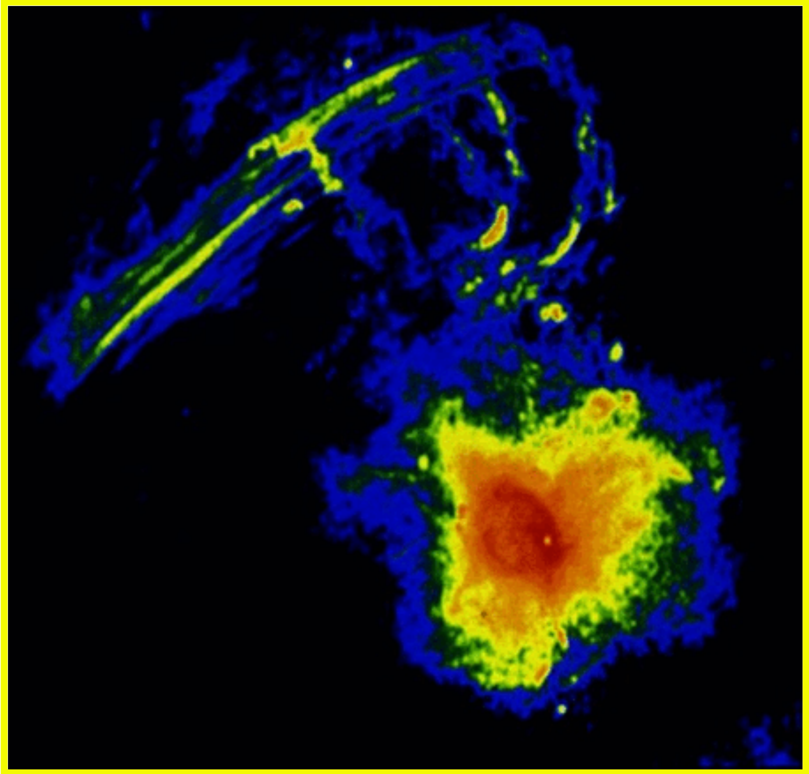

Radio Emission from Sgr A*

- Intrinsic dimension of Sgr A*, measured at 43 GHz (Bower et al. 2004) compared to the horizon dimension of the central BH
- The radio source measures ~1 AU

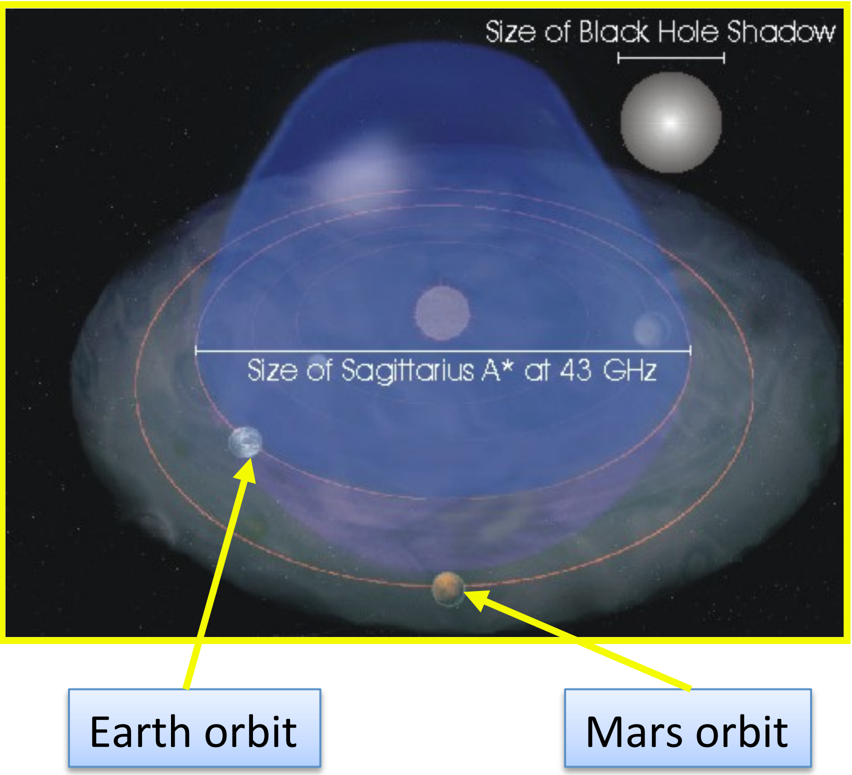

Ionized gas H92α near Sgr A*

- Close-up of Sgr A* showing the mini spiral of ionized gas falling onto the BH
- The bright spot is Sgr A*, corresponding to the BH

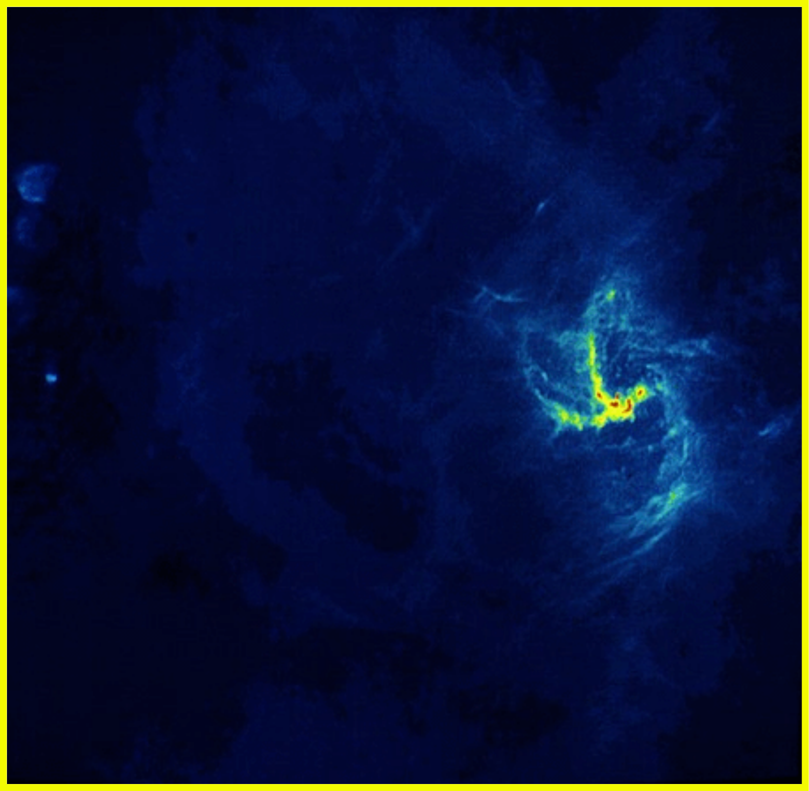

X-ray emission (Chandra) Sgr A*

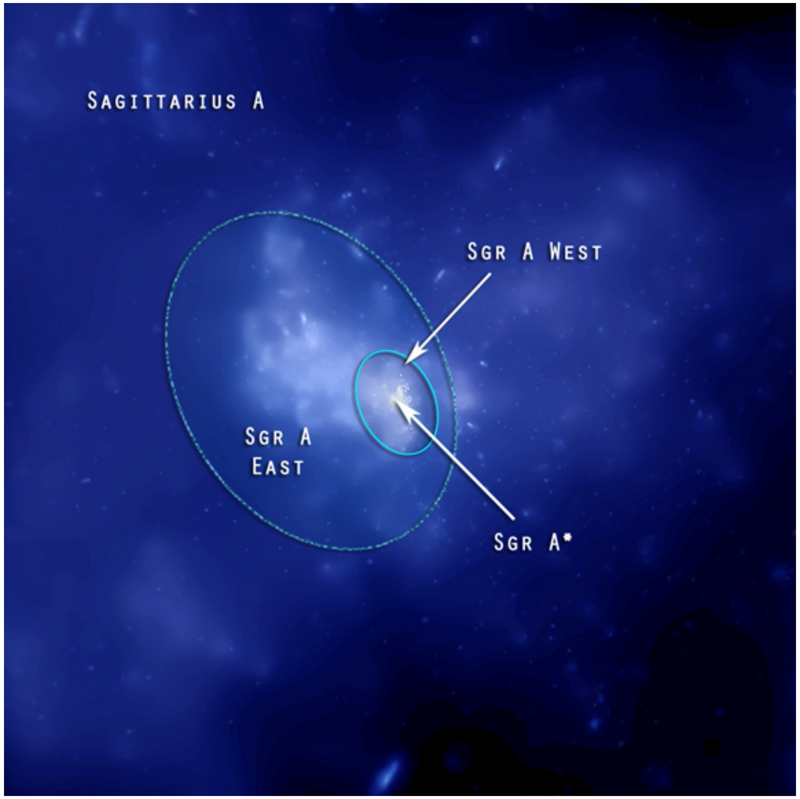

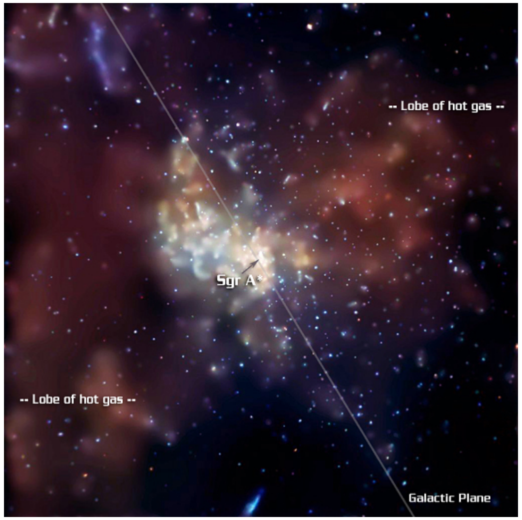

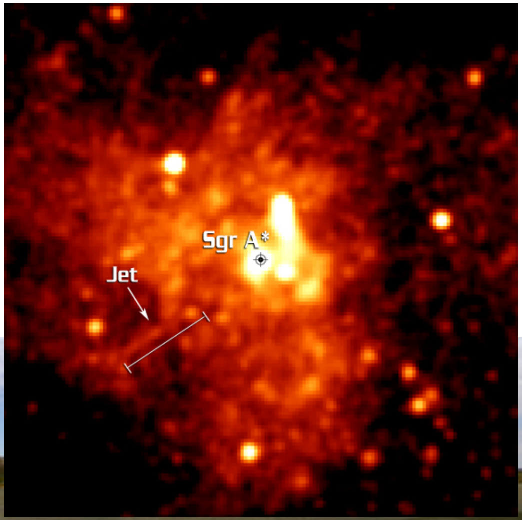

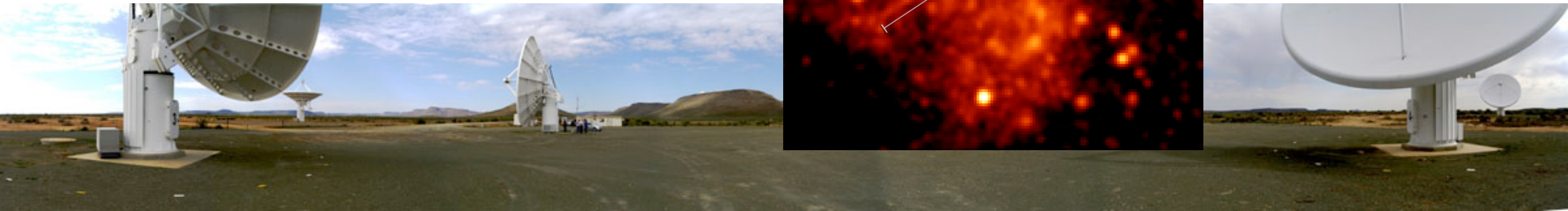

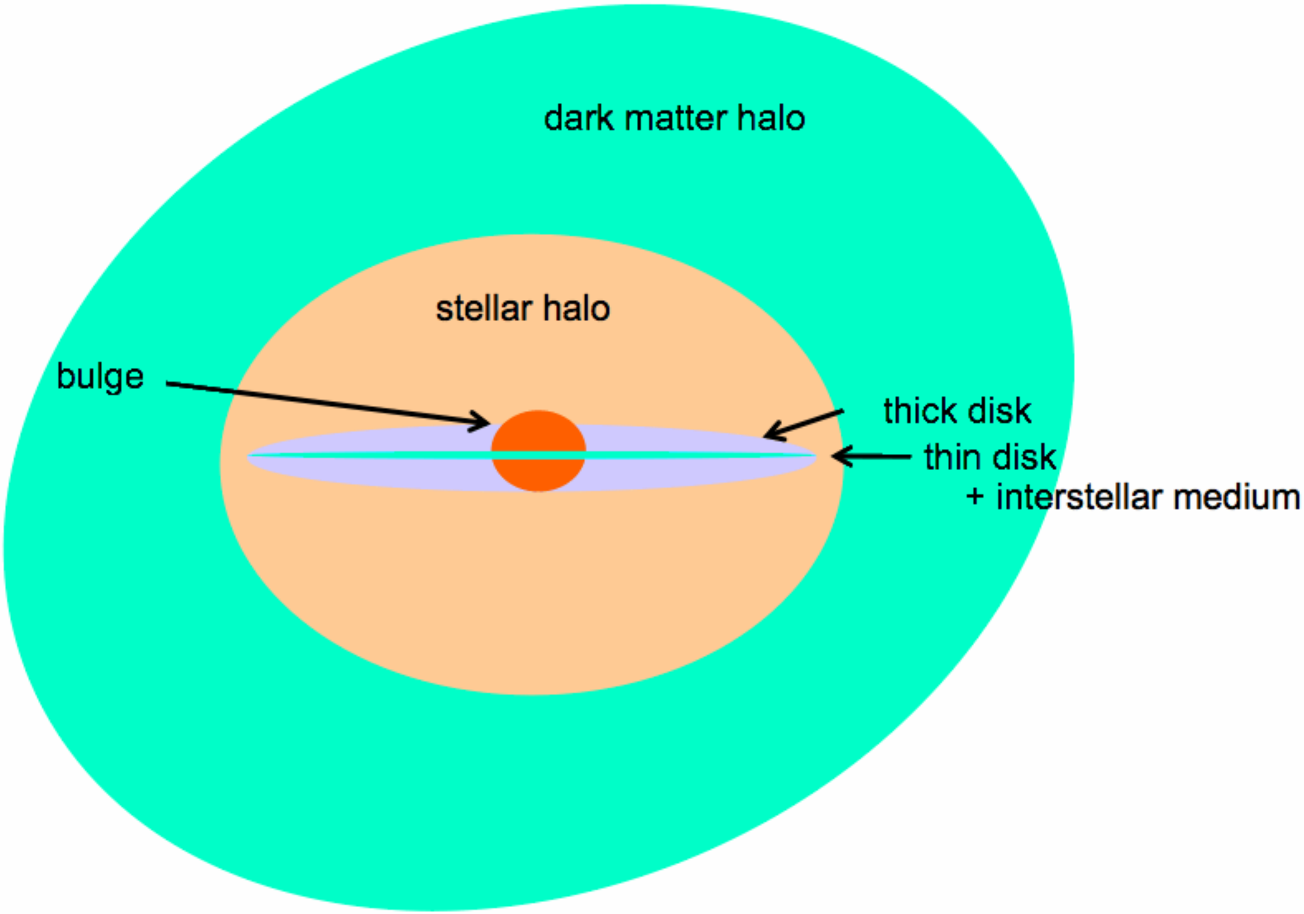
dark matter halo
stellar halo
bulge
thick disk
thin disk
+ interstellar medium

Thin disk vs Thick disk

- Thin disk: main stellar component
  - Young thin disk with a mean [Fe/H] ~ 0.0 and an exponential scale height h_z ~ 100 pc (with HI & H_2)
  - Old thin disk with a mean [Fe/H] ~ -0.3 and an exponential scale height h_z ~ 300 pc

Thin disk vs Thick disk

- Thick disk: second stellar component (Gilmore & Reid 1983):
  - ➢ Exponential scale height $h_z \sim 500\text{-}1400$ pc
  - ➢ Velocity dispersion much larger than for the thin disk
  - ➢ Less metals than the thin disk $-2.2 <$ [Fe/H] < -0.5

Disk Galaxy

- Surface brightness distribution in R:

  $\mu(R) = \mu_0 e^{-\alpha R}$ $\quad I(R) = I_o \exp(-R/h)$

- I_o, the central surface brightness is (μ_{0B} ~ 21.65 mag arcsec^{-2}): $140\ L_\odot\ \mathrm{pc}^{-2}$
- h (α^{-1}) *scale length*:
  - 3-4 kpc for a galaxy similar to the MW
  - 1.5 kpc for a galaxy similar to the LMC
- Surface brightness distribution in z:

$$L(R,z) = \begin{cases} L_0 e^{-R/h}\ \mathrm{sech}^2\ (z/z_0) & R < R_{\max} \\ 0 & R > R_{\max}. \end{cases}$$

- z_0 scale height ~ 0.5-1.0 kpc

Halo: globular clusters

Globular cluster distribution about the galaxy (black dots)

Plotted on top of the COBE FIRAS 2.2 micron map in Mollweide projection

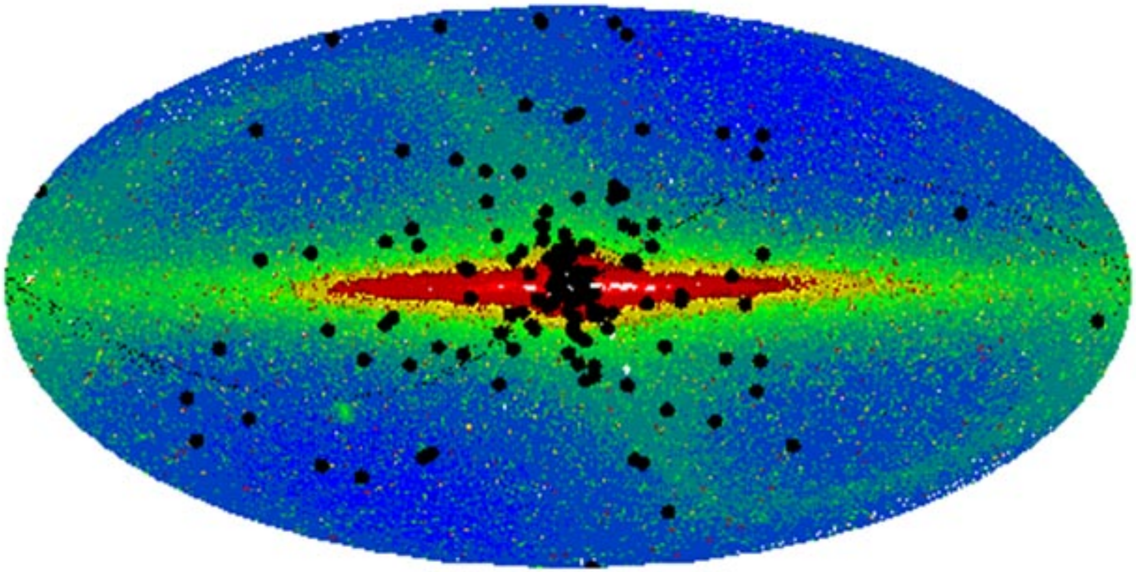

Halo: globular clusters

- Globular clusters would be coming from gas clouds gravitationally bound before the galaxies formed
- Present day cosmological theories (e.g. ΛCDM) predict that the first structures that formed would have been gas clouds (in the potential well of dark halos) with masses similar to globular clusters
- Globular clusters are indeed the oldest structures in the Universe

Halo: globular clusters

Main characteristics:

- Number of stars: 10^4-10^6
- Central density: 10^3-10^4 M_{sun} pc^{-3}
- Number: ~150 around the MW with ~20% at a few kpc of the GC
- Only 2% of the light and of the stellar mass of the halo
- Oldest GC ~ 13 +/-2 Gy in the outer halo (close to the lower limit of the age of the Universe)

Halo: globular clusters

- The ages of the oldest GC of the inner and outer halo, the LMC, the dSphs Fornax and Sagittarius are similar to within ~ +/- 1 Gy
- This means that the formation process of the GCs was well synchronize in a volume centered on the MW > 100 kpc
- GCs are older than the oldest stars in the disk (WD and old RG)
- GCs are poorer in metals that the underlying halo light in all galaxies and at all radii.

Halo: globular clusters

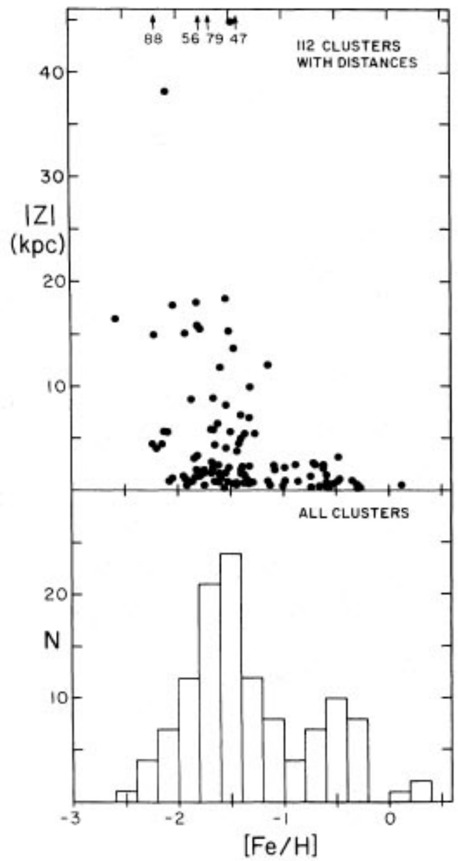

FIG. 1.—In the upper diagram, |Z| is plotted against [Fe/H] for the 112 globular clusters of known distance. Notice that there are no clusters in the zone 20 ≲ |Z| ≲ 37 kpc and that the |Z| distribution changes suddenly at [Fe/H] ≈ −1. The lower diagram is a histogram of the values of [Fe/H] for all 121 clusters in Table 1. Notice that the valley in the distribution over [Fe/H] occurs at the same value as the sudden change in the |Z| distribution.

- Kinematics & metallicity distributions: there is 2 populations
- Metal-poor [Fe/H] < -0.8, halo population, rotate slowly & spherically distributed
- Metal-rich [Fe/H] > -0.8, disk population, rotate rapidly & flattened distribution

Halo: globular clusters

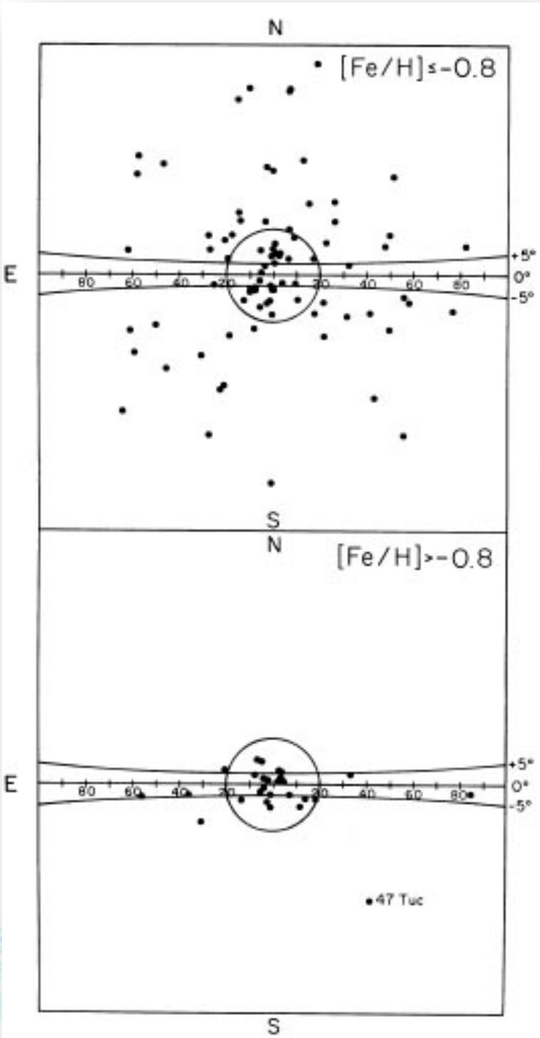

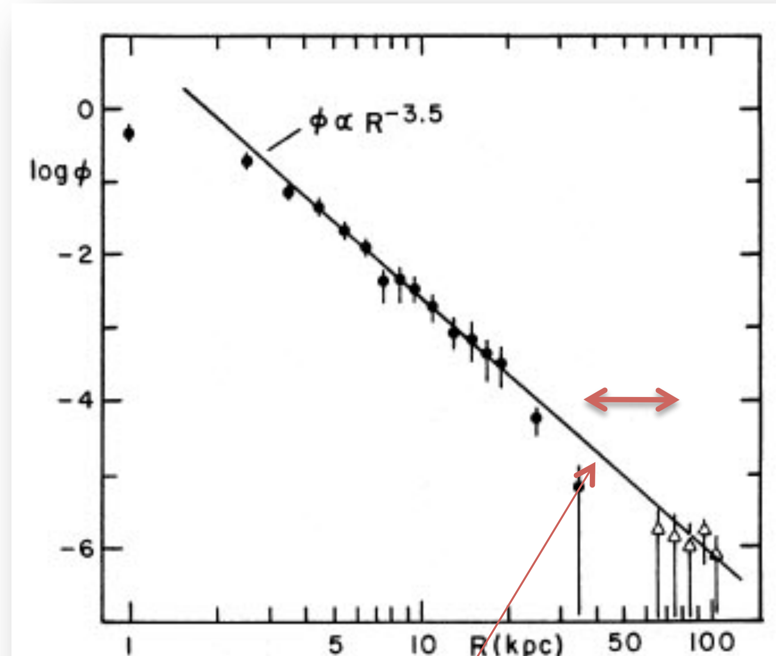

FIG. 2.—The number of clusters per cubic kiloparsec (ϕ) is plotted against galactocentric distance (R). The solid circles represent the clusters with $|Z| < 20$ kpc; the open triangles represent the clusters with $|Z| > 37$ kpc. There are no clusters in the zone $33 < R < 60$ kpc.

Halo: globular clusters

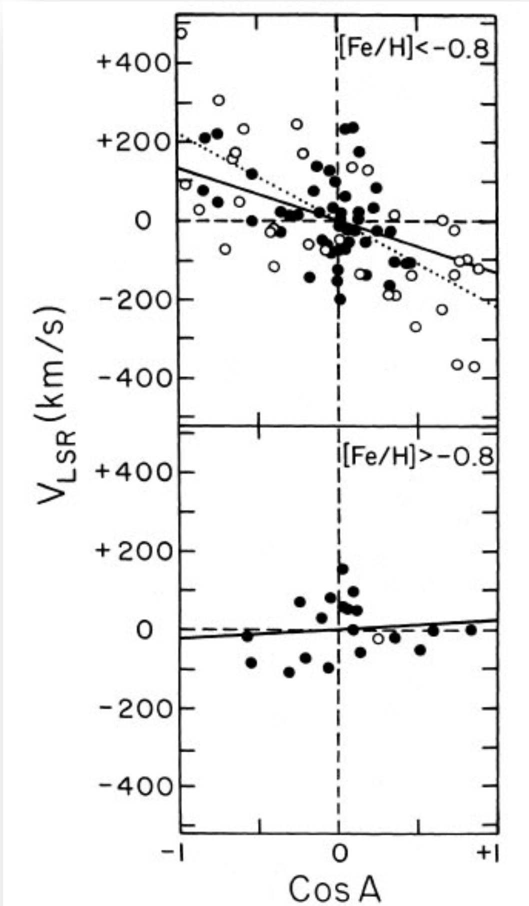

FIG. 6.—The radial velocities of the clusters with respect to the Local Standard of Rest (V_{LSR}) are plotted against the cosine of the angles (A) between their positions on the sky and the apex of the motion of the LSR. Solid circles denote the clusters that have $R < R_{\odot}$. The solid lines are least square fits to these data. Open circles denote the clusters that have $R > R_{\odot}$, and they are fitted by the dotted line. The fitted lines in these diagrams yield the values of U and σ given in Table 5.

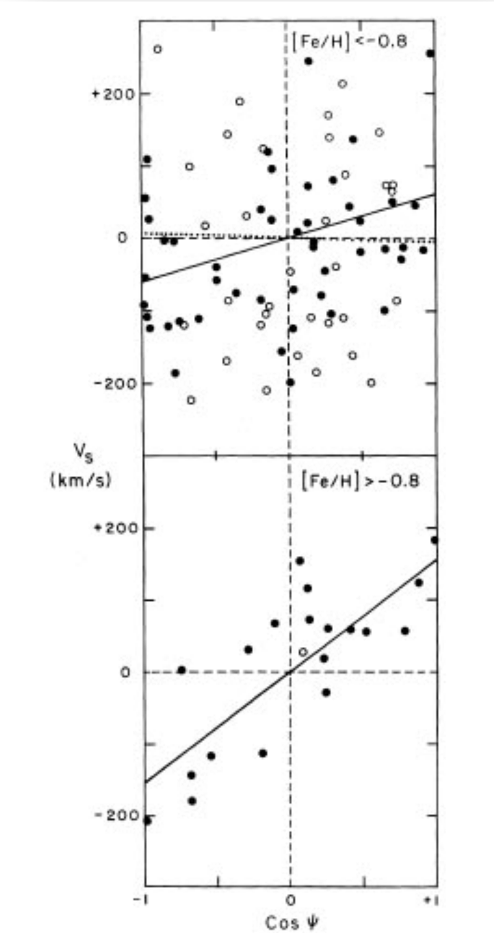

FIG. 7.—The radial velocities of the clusters as seen by an observer who is at rest with respect to the galactic center (V_s) are plotted against the cosine of the angles (ψ) at the clusters between the direction to the observer and the rotational velocity vectors of the clusters. The symbols have the same meanings as in Fig. 6. The solid and dotted lines were fitted to the solid and open circles, respectively. They yield the values of v_{rot} and σ that are given in Table 7.

Halo: globular clusters

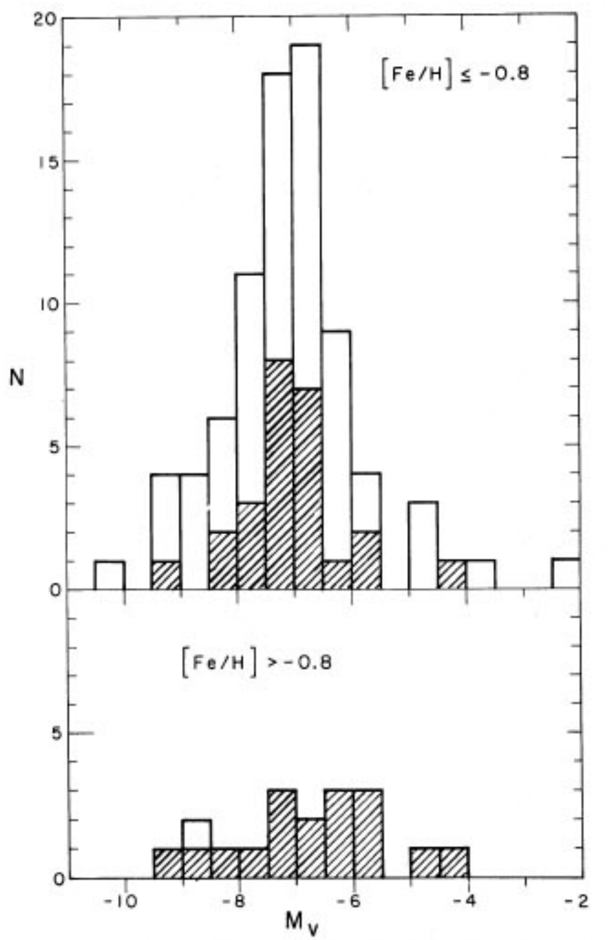

FIG. 10.—The luminosity functions of the halo (*top*) and disk (*bottom*) clusters. The shaded histograms are the luminosity functions of the clusters that have $|b| < 11°$.

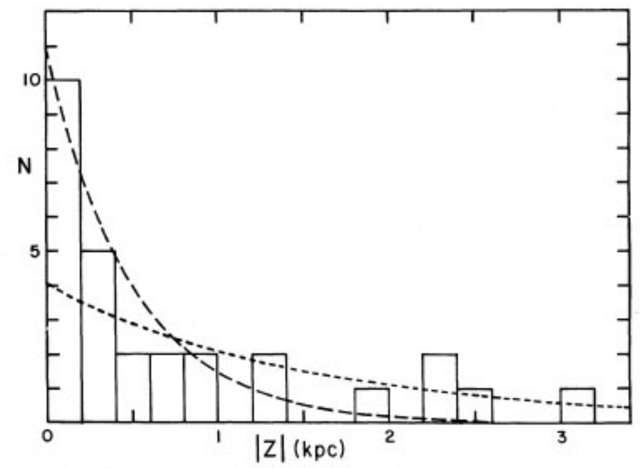

FIG. 9.—The $|Z|$ distribution of the disk clusters. The long-dashed and the short-dashed curves are exponentials with a scale heights of 500 and 1500 pc respectively.

Halo: globular clusters

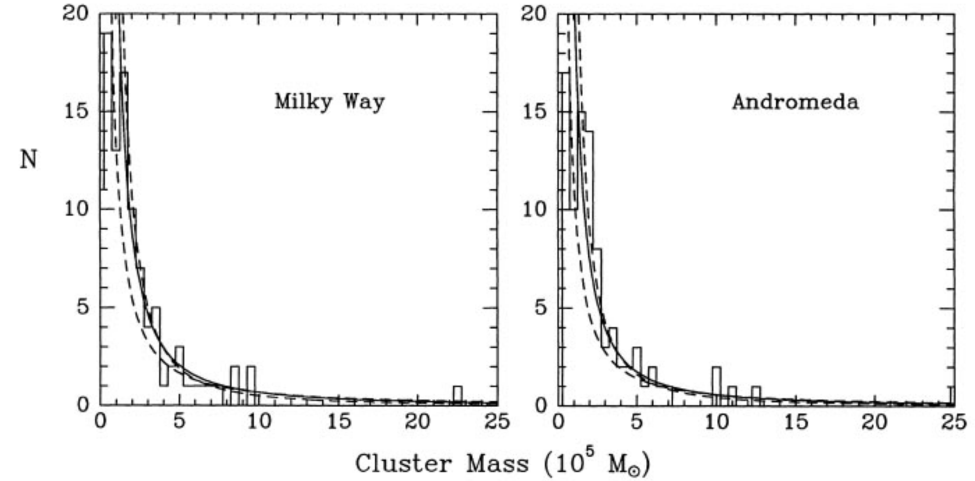

FIG. 1.—(*left*) Mass distribution for the globular clusters in the Milky Way halo, with data as listed by Secker (1992). Here N is the number of clusters per 0.5×10^5 $M_\odot$ bin. The *solid line* is the power-law mass distribution $N \sim M^{-\alpha}$ with $\alpha = 1.6$ (see § 2 of the text). The dashed lines show similar fits for $\alpha = 1.3, 1.9$. (*Right*) The mass distribution for a complete sample of globular clusters in the M31 halo. The fitted curves are the same as for the Milky Way.

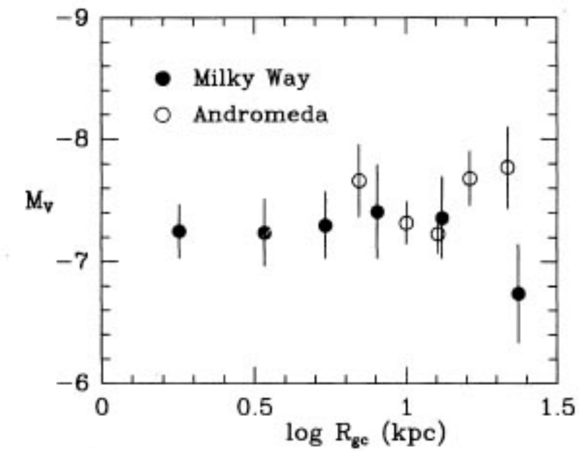

FIG. 6.—Mean absolute magnitudes $\langle M_V \rangle$ of the globular clusters in the Milky Way and M31, as a function of galactocentric distance. The data for the individual clusters are the same as used in Fig. 1 and § 2 of the text. Each plotted bin contains 15–20 clusters. For $R_{gc} \lesssim 30$ kpc, no dependence of mean luminosity on location is seen.

- GCs MW vs M31 (Harris & Pudritz 1994)

Halo: globular clusters

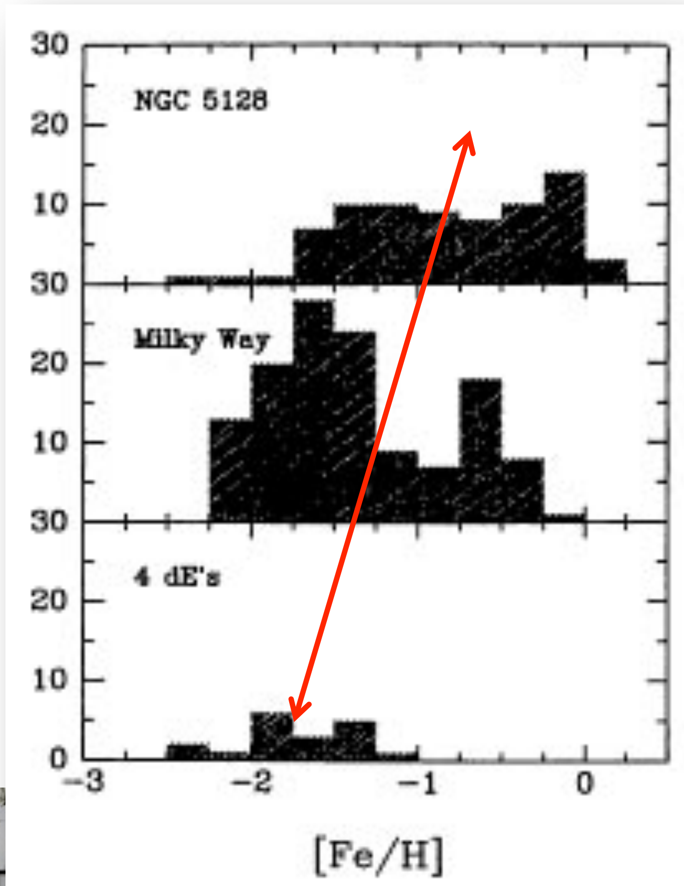

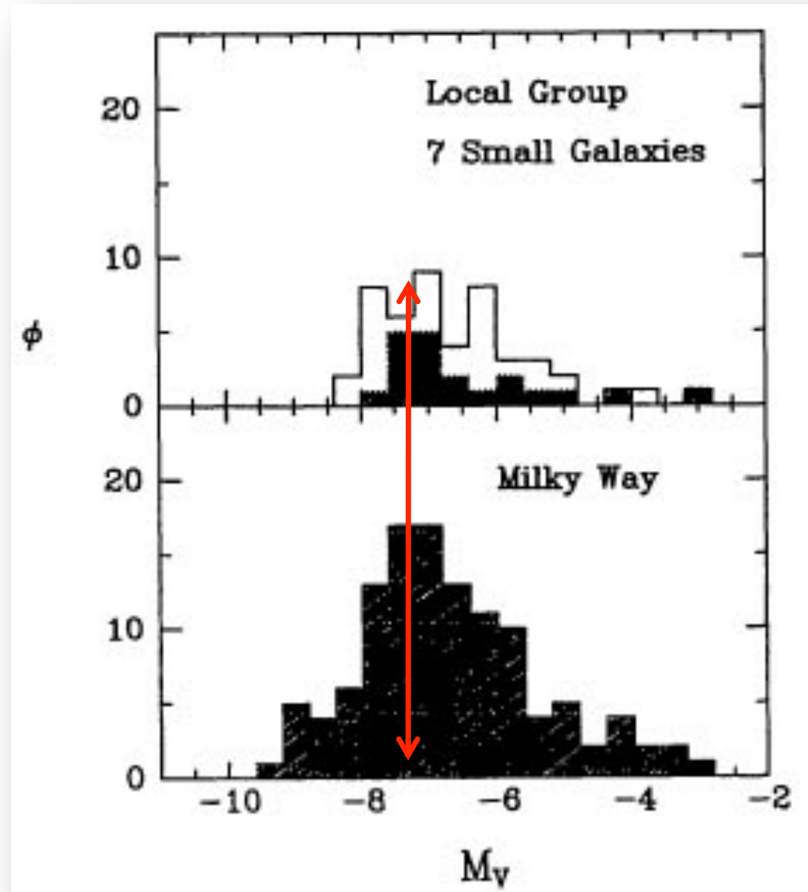

Halo: globular clusters

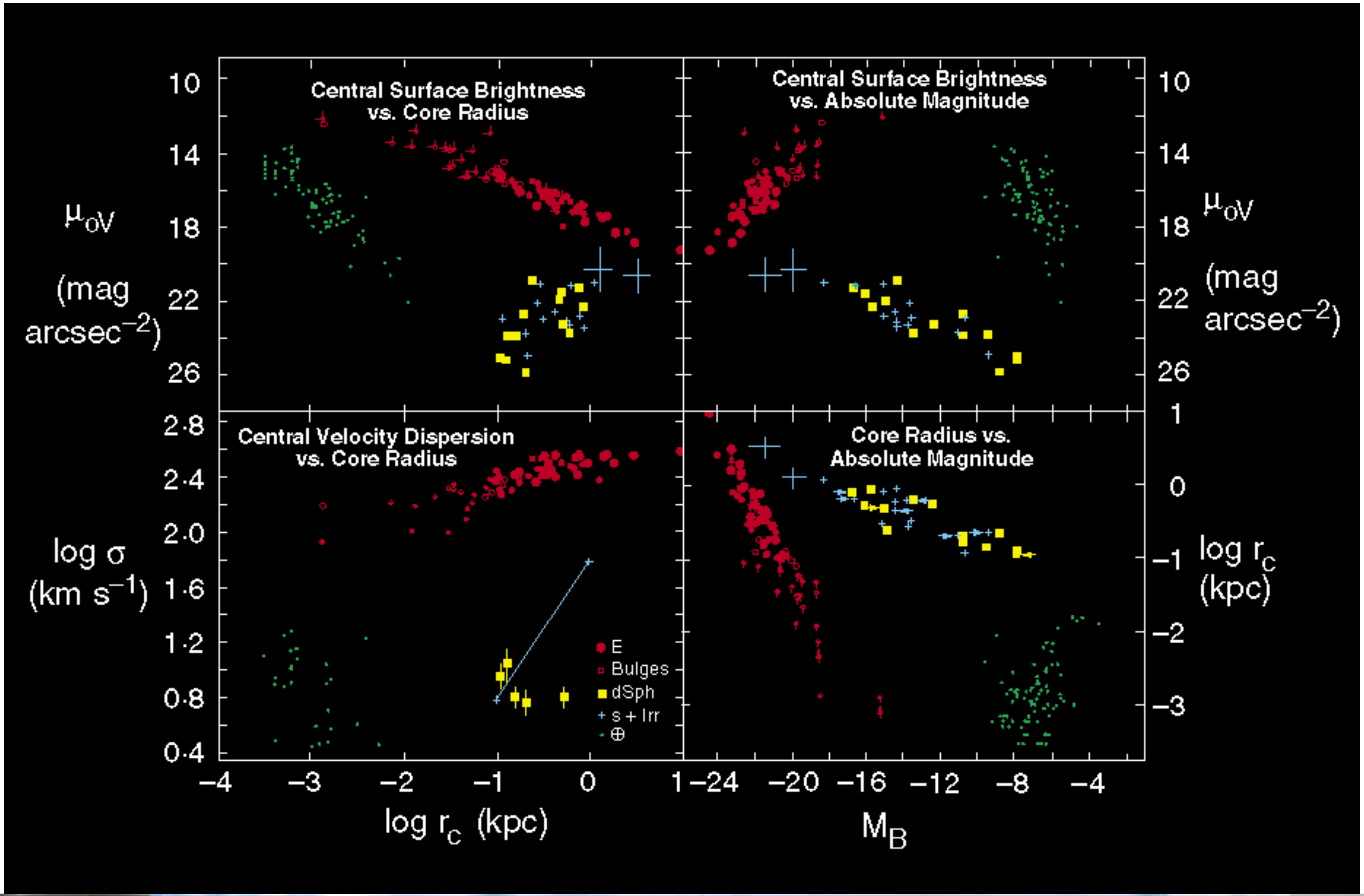

Halo: globular clusters

- As mentioned, it is possible that some GCs formed through mergers: This could explain:
  - ➢ The disk population of GCs
  - ➢ The excess of GCs around ellipticals (produced by mergers) as compared to spirals
  - ➢ The abnormally large number of GCs around certain galaxies (e.g. M87 – cD)

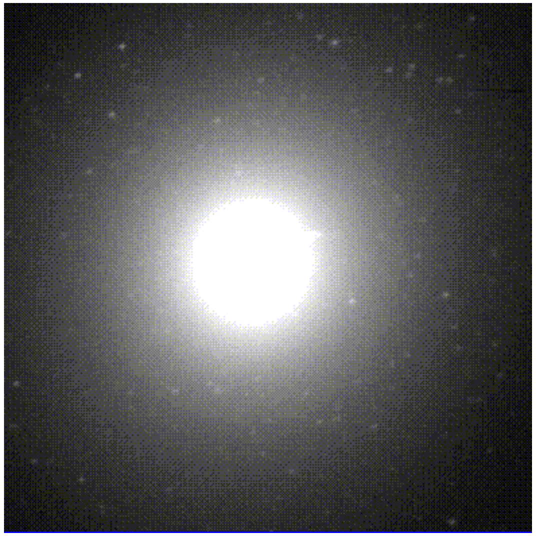

M 87

Halo: globular clusters

- NGC 1275 (HST)
- Mv ~ -12 to -14
- Blue (V-R) < 0.3
- $M_{GCs} \sim 10^5 - 10^8\ M_{sun}$
- Merger of NGC 1275 ~ 10^8 y

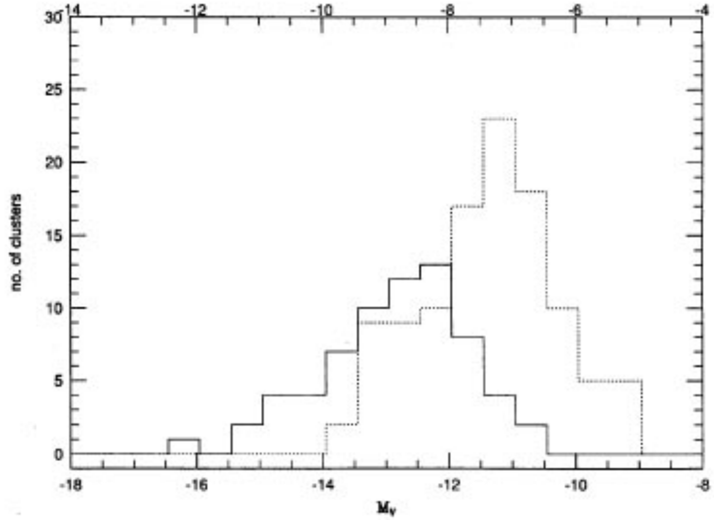

FIG. 7. The luminosity function of cluster objects. The dotted line shows the luminosity function for Milky Way globulars. The current absolute magnitude for the NGC 1275 objects is shown on the bottom scale. The top scale is relevant for the Milky Way clusters, and is the prediction for the NGC 1275 clusters if they were to fade by 4 mag.

Halo: globular clusters

NGC 7252 - HST

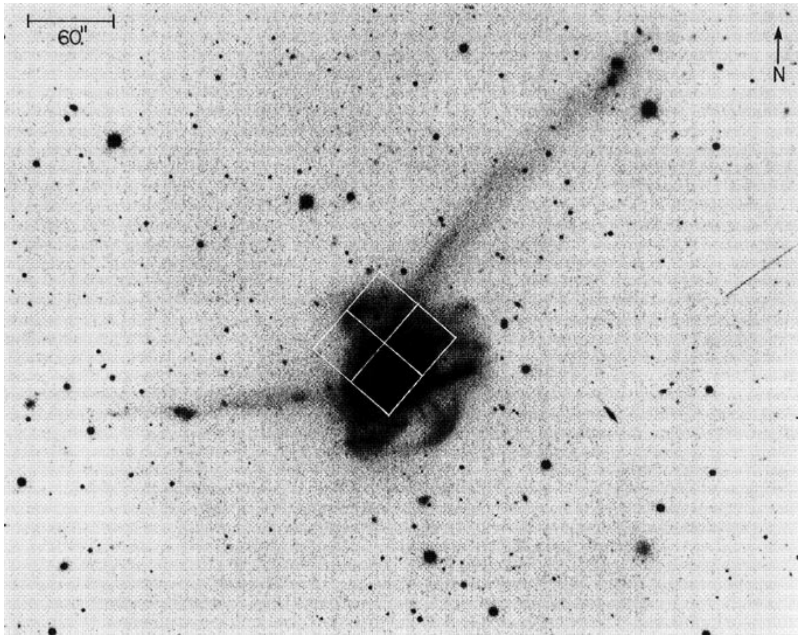

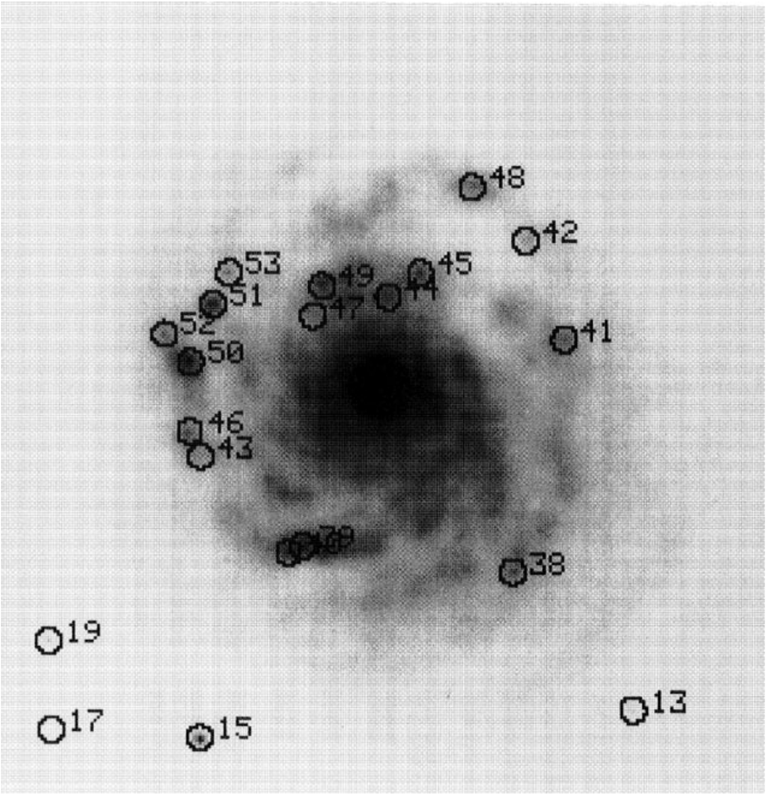

Whitmore et al. 1983

Halo: globular clusters

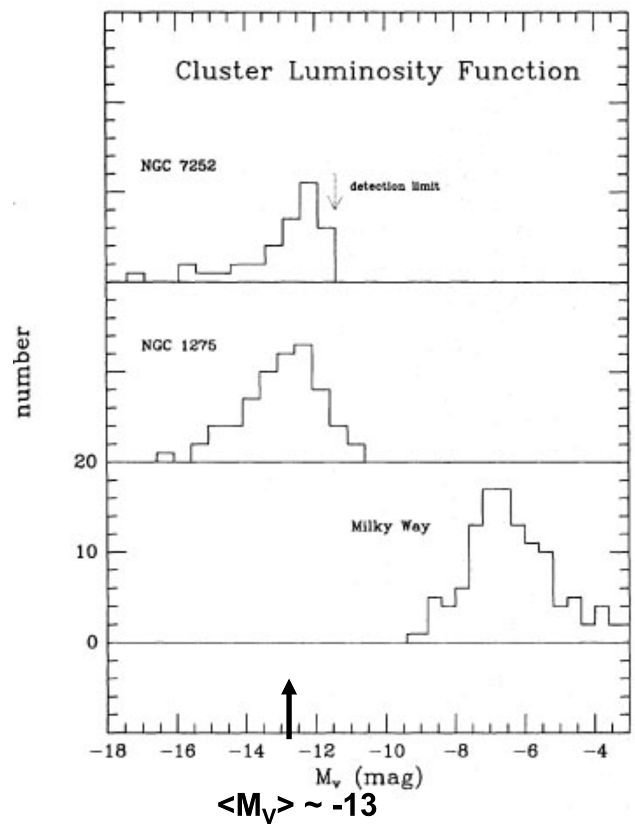

FIG. 8. The luminosity histogram for the objects in the outer sample of NGC 7252, NGC 1275 (H92; correction of 0.75 mag has been applied based on "note added in proof"), and the Milky Way (Harris 1991).

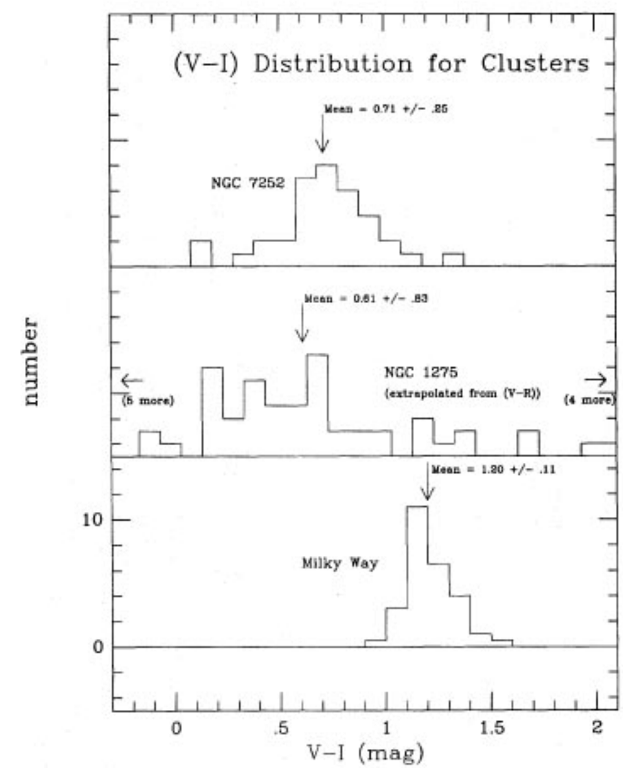

FIG. 9. The $V-I$ distribution of the objects in the outer sample of NGC 7252, NGC 1275 (H92; extrapolated from their $V-R$ values), and the Milky Way (Harris 1991). Reddening corrections of 0.12 and 0.27 mag have been made to the NGC 7252 and NGC 1275 data, respectively (see text).

Whitmore et al. 1983

Halo stars

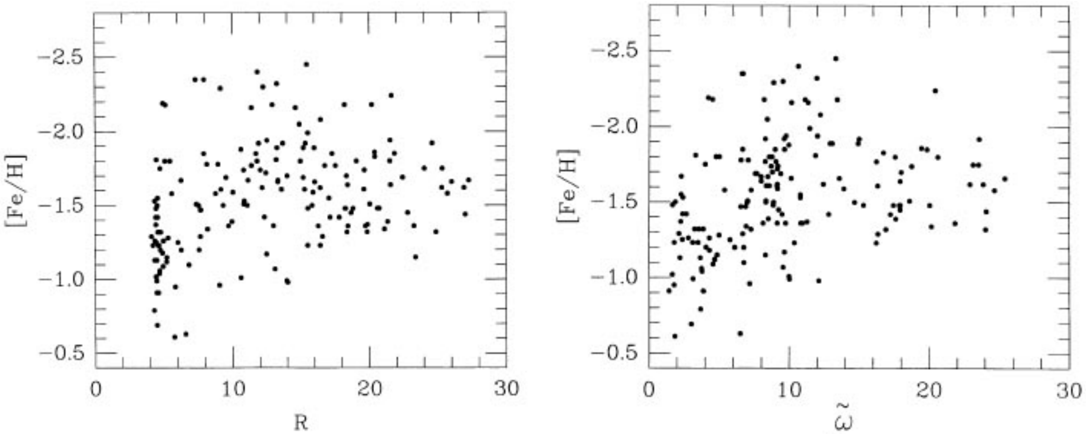

FIG. 3a FIG. 3b

FIG. 3.—[Fe/H] as a function of distance from the Galactic center for the 171 stars in the Lick surveys and the Saha (1984) survey. A distance of 8.5 kpc to the Galactic center was used. (a) Abundance as a function of galactocentric distance R; (b) the same data as a function of ϖ, the galactocentric distance projected onto the plane of the Galaxy. The spread in abundance at any given distance reflects an intrinsic spread of about 0.3 dex in [Fe/H] in the population of RR Lyrae variables. There is a noticeable nonzero gradient in the population for distances out to about 10 kpc, after which the gradient is zero.

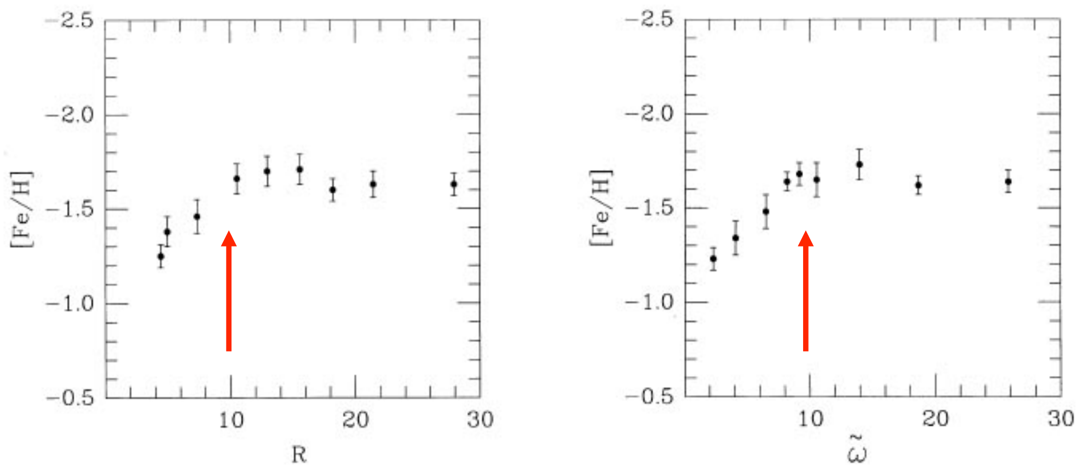

Gradient
0 < R < 10 kpc
Constant
R > 10 kpc

Halo stars

TABLE 7

AVERAGE [Fe/H] FOR FIELD RR LYRAE VARIABLES AND GLOBULAR CLUSTERS

R (kpc)	$\langle$[Fe/H]$\rangle$	σ	Median [Fe/H]	N	$\langle R \rangle$ (kpc)
Globular Clusters					
4–5	−1.39	0.32	−1.39	10	4.3
5–8.5	−1.61	0.31	−1.60	16	6.4
4–8.5	−1.53	0.33	−1.58	26	5.6
RR Lyraes					
4–5	−1.27	0.30	−1.24	32	4.6
5–8.5	−1.45	0.45	−1.07	26	6.6
4–8.5	−1.35	0.38	−1.29	58	5.5

- Clearly, GCs are poorer in metals and older

Halo stars

Halo characteristics from HB stars:

- $\rho(r) \sim r^{-3.5}$ ($r < 25$ kpc) – similar to GCs
- $L_V/L_{Sun} \sim 4 \times 10^7$ (with $M/L_V \sim 2.5$ – GCs)
- $M_{halo} \sim 1 \times 10^8\ M_{sun}$
- $\sigma_R \sim 135$, $\sigma_\phi \sim 105$, $\sigma_z \sim 90$ km s^{-1}

Halo stars

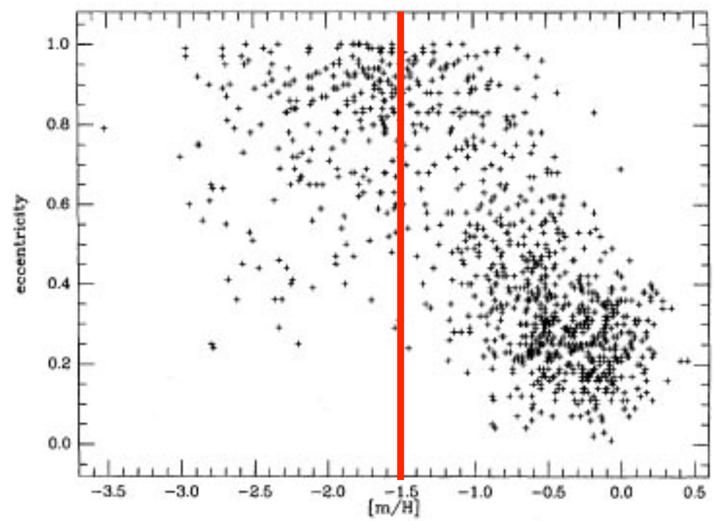

FIG. 2. The Galactic orbital eccentricities of the 1022 stars are plotted as a function of stellar metallicity.

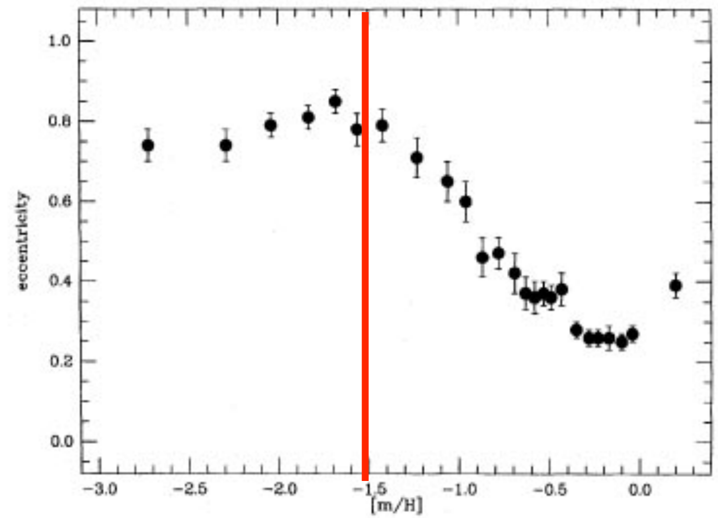

FIG. 4. Mean values in equal-size bins for the data in Fig. 2.

- 2 populations:
  1. Metal-poor & dynamically hot (no correlation)
  2. Metal-rich & dynamically cool (disk-like) (correlation)

Halo stars

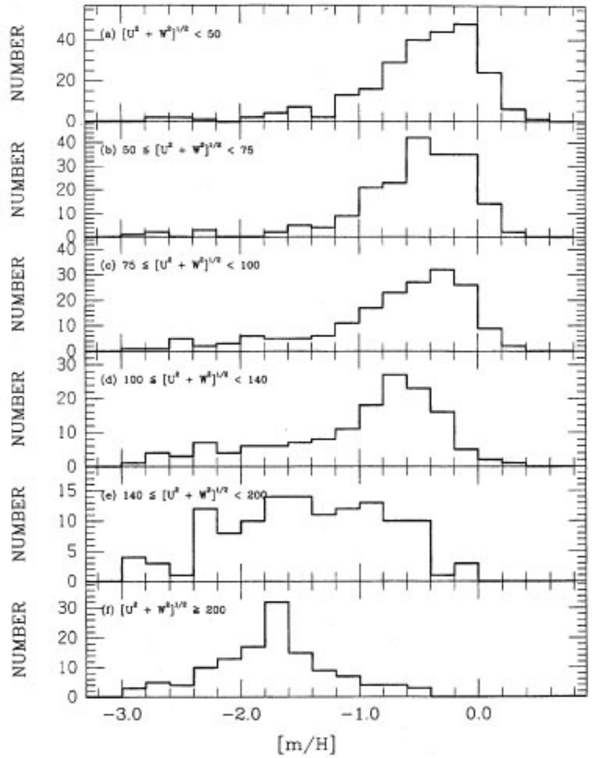

FIG. 6. Metallicity histograms for various $[U^2+W^2]^{1/2}$ velocity regimes.

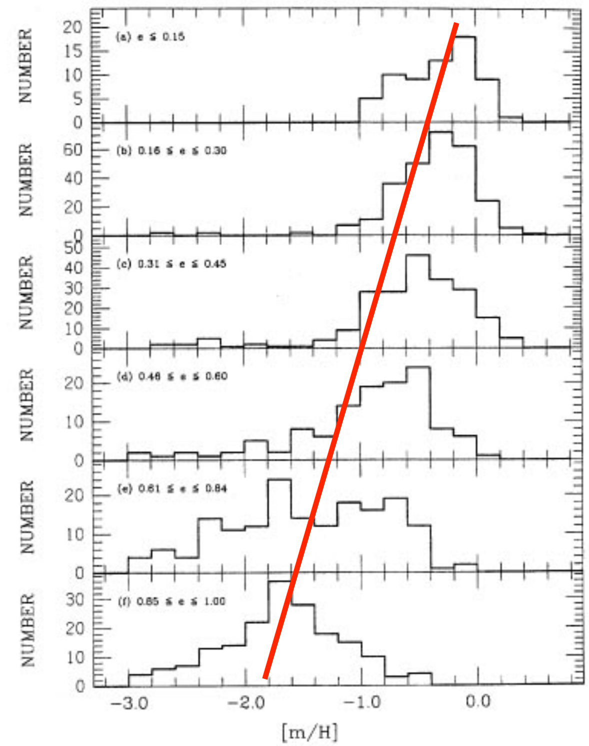

FIG. 7. Metallicity histograms for various Galactic orbital eccentricity regimes.

Origin of the halo

- Hyp.: the stellar structures that extend to 100 kpc consists of stars pulled out during the numerous mergers which characterize the hierarchical formation of galaxies
- The external luminous halos should show as an excess of luminosity above the extrapolation of the inner profile of the galaxy
- Densité: $\rho \sim r^{-3}$ (disk edge) & $\rho \sim r^{-4}$ (tidal radius) – mean: $\rho \sim r^{-3.5}$
- Luminous halos should have a similar form than the dark halos
- Most of the halo stars formed in progenitors which merged with the central galaxy

Origin of the halo

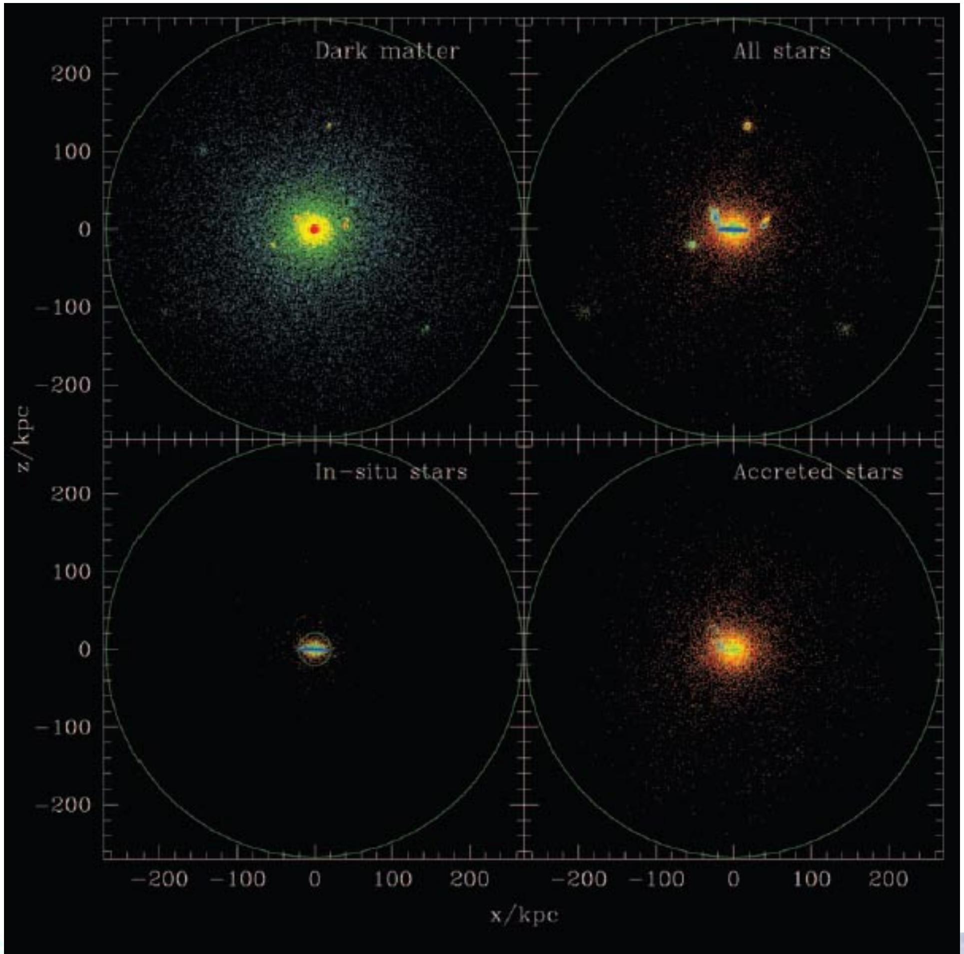

Abadi, Navarro & Steinmetz 2006

- Simulated galaxy at z=0
- Mass for $r < r_{viriel}$
- Stars:
  - Blue 0.0 < age < 2.5 Gy
  - Red 10 < age < 15 Gy
- External circle = R_{viriel}
- Internal circle = R_{lum}

Origin of halo

$$\Sigma_c\ (M_\odot\ \mathrm{pc}^{-2}) = 0.59\alpha V\ (\mathrm{km\ s}^{-1})/R\ (\mathrm{kpc})$$

$\alpha \sim 1$

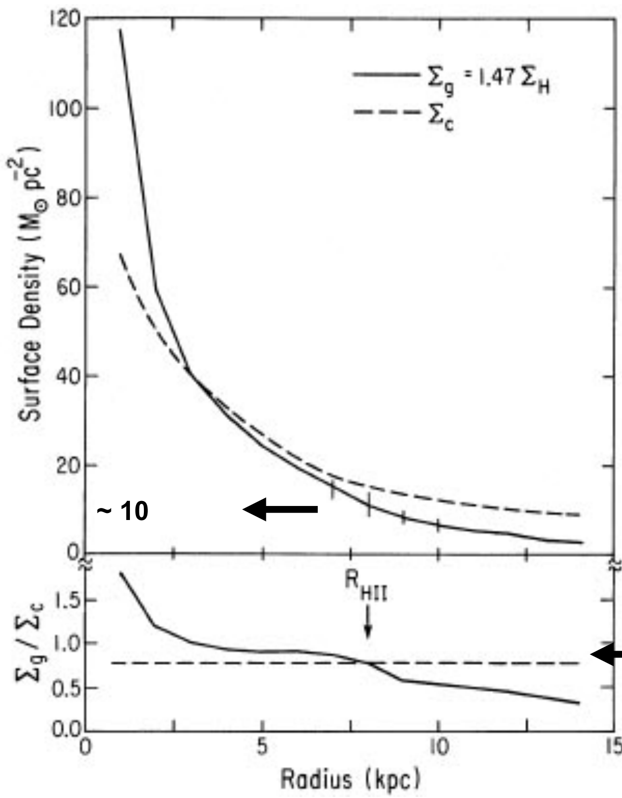

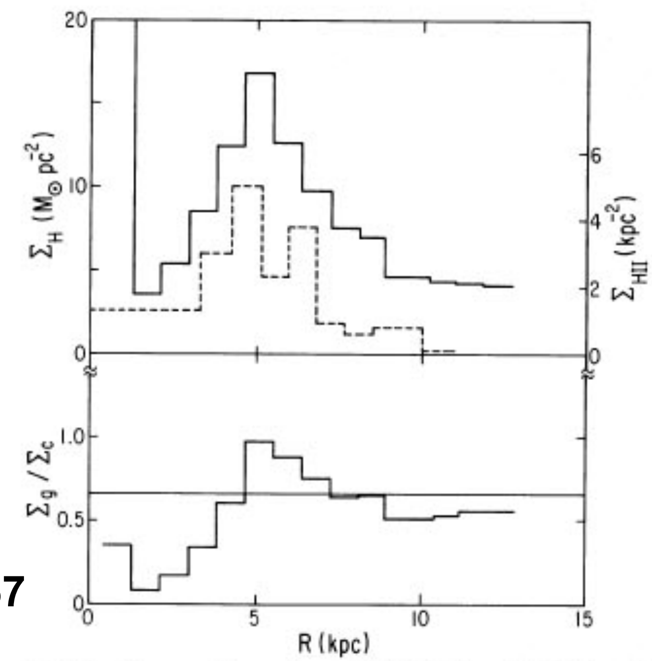

FIG. 16.—Top panel shows the radial distribution of total (H I + H$_2$) hydrogen surface density in the disk of the Milky Way Galaxy (*solid line*), and the surface density of giant H II regions (*dashed line*). Bottom panel shows the radial behavior of the ratio of gas density to the critical density for gravitational stability, as in Figs. 11 and 13.

$\Sigma_g = \Sigma_{HI} + \Sigma_{H_2}$

Kennicutt 1989

Origin of halo

Late-type

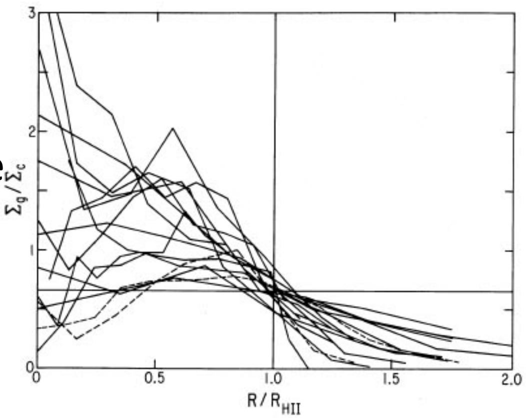

FIG. 11.—Radial dependence of the ratio of gas surface density to the critical density for gravitational stability (eq. [4]), for the galaxies with active star-forming disks. The radial coordinate is normalized to the radius of the H II region disk. The horizontal line indicates the value for the stability parameter ($\alpha = 0.67$) which best fits the observed star formation thresholds. Dashed lines denote M33 and NGC 2403.

Early-type

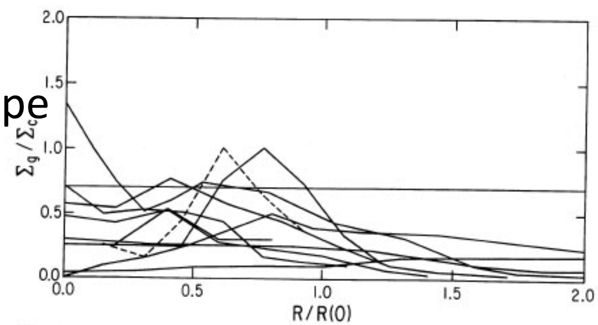

FIG. 13.—Radial behavior of the ratio of total gas surface density to the critical density for gravitational stability (eq. [4]), for early-type (Sab–Sbc) galaxies. The radial coordinate is normalized to the isophotal radius of the disk. The horizontal line indicates the value $\alpha = 0.67$ which best fits the observed star formation thresholds in late type galaxies. The dashed line denotes NGC 4548.

- The halo stars can not have been formed in situ since the gas density was below the threshold for SF
- They were ejected of galaxies during the mergers that characterized the assembly of galaxies by hierarchical clustering

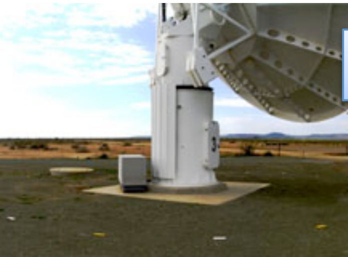

Kennicutt 1989

Origin of halo

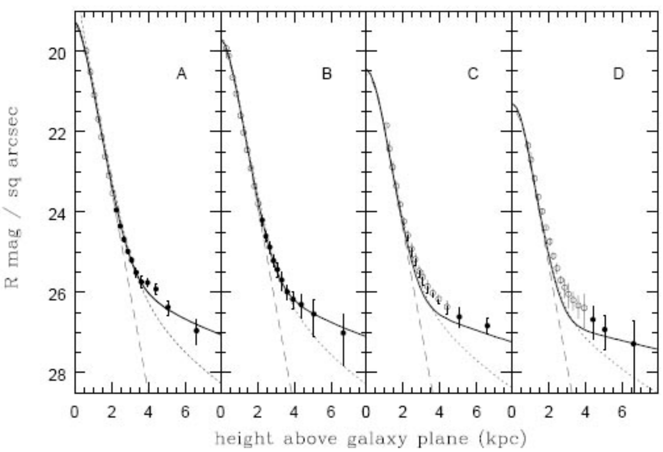

Fig. 1.— The total surface brightness in R mag arcsec^{-2} is shown as a function of distance from the galactic plane of NGC 5907 for four different cuts (spaced 4.1 kpc apart) perpendicular to the galactic plane. Positions of the cuts are shown in Figure 2(a). For each profile, light from matching positions in the four quadrants is averaged. Error bars include differences between quadrants as well as individual errors. Distances are in kpc and assume a distance of 11 Mpc to the galaxy. Open symbols denote areas underneath the mask shown in Figure 2, which do not contribute to the halo fit; closed symbols indicate unmasked areas. The dashed line shows the best fit to the total projected light using a thin, exponential disk, with scale length 4.8 kpc, scale height 430 pc, central surface brightness of 19.2 R mag arcsec^{-2} and truncation radius of 19.5 kpc. To obtain the thin disk fit, the inner regions of the galaxy were masked to avoid contamination from dust[3]. Also shown are the best fit for disk plus $r^{-3.5}$ halo with a 200 pc core (dotted line), and disk plus $r^{-2.26}$ halo with a 2 kpc core (solid line).

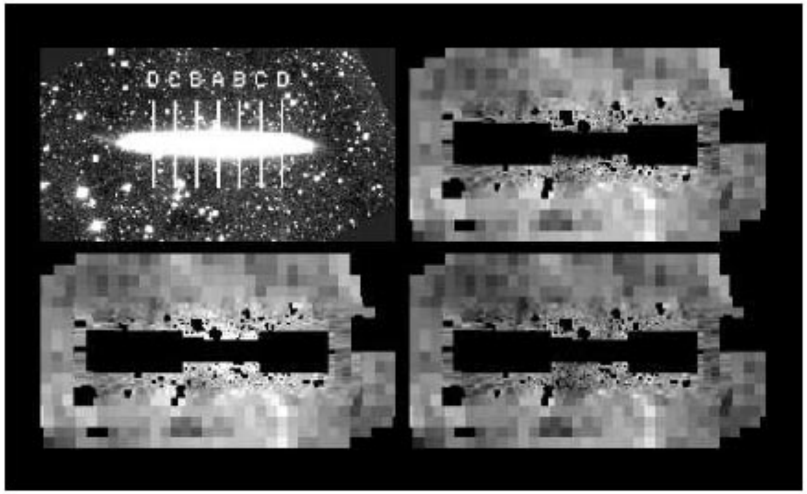

Fig. 2.— Optical image of NGC 5907 (top left) and weighted residual images for three models. The area shown in each frame is slightly less than one-half the total usable detector area. Light areas indicate regions of excess light compared to the given model; dark areas indicate regions of insufficient light; black shows regions that have been masked due to confusion from dust, foreground stars, and warp. The data have been binned into $4'' \times 4''$ bins near the galaxy and $40'' \times 40''$ bins in the halo and sky regions in order to achieve similar signal-to-noise in each bin; thus each bin, regardless of its size, receives a similar weight in the fit. The residuals are expressed in terms of the uncertainty in each bin: white indicates regions with light in excess of 4σ from the model and black indicates 4σ deficits of light. The masked region is 46 kpc long and 4.3 kpc wide at the minor axis. **(top left)** Greyscale R-band image with the placement of the vertical profiles shown in Fig. 1 superposed. The contrast has been adjusted so that the galaxy is "over-exposed"; essentially *all* light from the exponential disk is shown as pure white. **(bottom left)** Residuals from Thin Disk Only model. Disk parameters are given in the caption to Fig. 1. The strong positive residuals indicate the presence of extended halo light. Reduced χ^2 for this fit is 6.0. **(top right)** Residuals from Thin Disk + $r^{-3.5}$ Halo model. Disk parameters are given in the caption to Fig. 1; halo has $c/a = 0.27$ and a core radius of 200 pc. Reduced χ^2 for this fit is 2.3. **(bottom right)** Residuals from Thin Disk + Free Power Law Halo model. Disk parameters are unchanged; halo has an exponent of -2.26, $c/a = 0.53$, and a core radius of 2 kpc. Reduced χ^2 for this fit is 1.5.

Sackett et al. 1994

Mass of the halo (dark)

$$M_{\text{est}} = \left(\frac{2}{\langle e^2 \rangle_s}\right)\left(\frac{1}{GN}\sum_{i=1}^{N} v_{ri}^2 r_i\right)$$

=1 : radial orbits
=1/2 : isotropic orbits

Data for Sample Objects[a]

Object	(l, b)	r	$r_\odot$	References	v_r^{iso}	v_r^{rad}	$v_\odot$	Δv	References
LMC+SMC	(284, −36)	51	52	1	61	62	245	5	1
Ursa Minor	(105, 45)	65	63	1	−87	−88	−249	1	1
Draco	(86, 35)	75	75	1	−94	−95	−289	1	1
Sculptor	(288, −83)	79	79	1	74	75	107	2	3
Carina	(260, −22)	93	91	1	14	14	230	1	1
Fornax	(237, −66)	140	138	1	−34	−34	55	5	1
Leo II	(220, 67)	223	220	1	38	38	95	25	1
Leo I	(226, 49)	224	220	1	75	75	185	25	1
NGC 5694	(331, 30)	25	31	2	−238	−244	−152	4	4
NGC 6229	(74, 40)	31	32	2	22	23	−154	8	5
NGC 7006	(64, −19)	36	39	2	−166	−170	−364	10	4
Pal 3	(240, 42)	95	91	1	−60	−60	89	9	1
NGC 2419	(180, 25)	98	90	1	−26	−26	−20	5	1
Pal 4	(202, 72)	108	105	1	51	52	75	5	1
AM-1	(258, −48)	117	116	1	−42	−42	116	15	1

[a] The first eight objects are dwarf galaxies, while the last seven are globular clusters. Within each subgroup, entries are listed in order of increasing Galactocentric distance r. Coordinates are given in degrees, distances in kpc, and velocities in km s^{-1}.

References.—(1) OPA; (2) Webbink 1985; (3) Armandroff and Da Costa 1986; (4) Hesser, Shawl, and Meyer 1986; (5) Webbink 1981.

- Isotropic velocity distribution + 10 objects 50-140 kpc M ~ 2.4 +/- 1 x 10^{11} M_{sun}
- R_{halo} > 50 kpc

Mass of the halo (MW + M31)

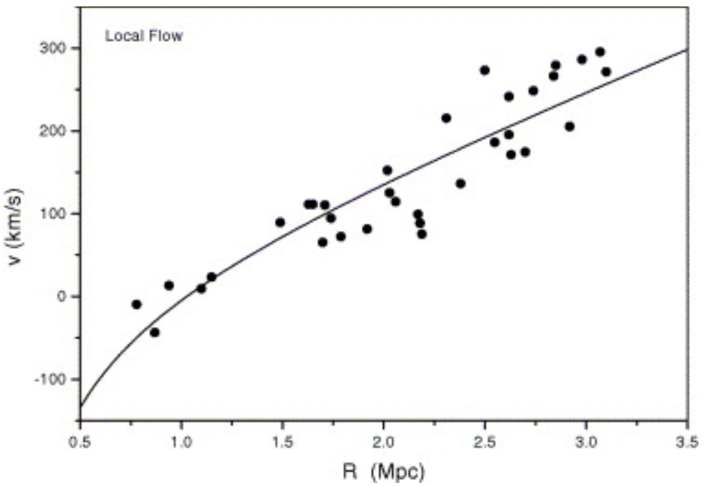

Karachentsev et al. 2002

$$M = 1.827 \frac{H_0^2 R_0^3}{G} = 4.1 \times 10^{12} h^2 R_0^3 \; M_\odot,$$

Turn-around radius

- Masse of the pair M31-MW = 2.5 +/- 0.7 x 10^{12} M_{sun}
- H_0 = 74 +/- 4 km s^{-1} Mpc^{-1}
- σ_{LG} = 39 km s^{-1}
- R_{bs} = 2.3 Mpc